To the Graduate Council:

I am submitting herewith a thesis written by Peter Demarest entitled "Aerodynamic Effects on an Earth Orbiting Satellite". I have examined the final copy of this thesis for form and content and recommend that if be accepted in partial fulfillment of the requirements for the degree of Master of Science, with a major in Aerospace Engineering.

Frank G. Collins

Frank Collins, Major Professor

We have read this thesis
and recommend its acceptance:

Ziqi Wu

Gary A. Flandro

Accepted for the Council:

C W Minkel

Associate Vice Chancellor and
Dean of The Graduate School

Aerodynamic Effects on an Earth Orbiting Satellite

A Thesis
Presented for the
Master of Science
Degree
The University of Tennessee, Knoxville

Peter Demarest
August 1996

DEDICATION

This thesis is dedicated to my grandmother

Mrs. Henrietta Shuart.

ACKNOWLEDGEMENTS

I would like to thank my advisor Dr. Frank Collins and the members of my committee, Dr. Jimmy Wu and Dr. Gary Flandro for their advise and guidance during the writing of this thesis. I would also like to acknowledge several other people who helped provide the resources that made this project possible. Dr. B. E. Schutz at the University of Texas for providing orbital data for the ERS-1 spacecraft. Mr. Don Shereda at Wright Labs for for providing the S/HAB Program. And Mr. Dave Rowen at Goddard Space Flight Center for supplying the GEODYN II Orbit Determination Program.

ABSTRACT

Satellites orbiting the Earth experience both a lift and a drag force due to the atmosphere. Historically, only the drag force has been investigated. Lift and drag forces are both related to the gas-surface interaction between the atmosphere and the satellite. This study hopes to show that an improved model of the gas-surface interaction using a variable model for the normal and tangential momentum accommodation coefficients can increase the accuracy of orbit prediction programs. The orbit of the ERS-1 satellite was analyzed by comparing changes in the semi-major axis and eccentricity of the orbit with predicted changes using the traditional diffuse model and the improved variable model for the accommodation coefficients. It was found that although the variable model predicts much a much greater lift force on the satellite, improved modeling of the atmospheric density is need to accurately predict orbital perturbations. A procedure for incorporating a lift model into an orbit prediction program is suggested.

TABLE OF CONTENTS

LIST OF FIGURES

NOMENCLATURE

a	Semi-Major Axis
a_e	Earth's Mean Equitorial Radius
a_p	Perturbing Acceleration
A_D	Acceleration Due to Drag
A_R	Accelration Due to Radiation Pressure
A_S	Cross Sectional Area of Satellite
C_D	Coefficient of Drag
C_L	Coefficient of Lift
C_{nm}	Gravitational Coefficient
C_R	Coefficient of Reflectivity
D	Drag Force
e	Eccentricity
E	Eccentric Anomoly
F_n	Normal Force
F_r	Radial Force
F_t	Tangential Force
G	Universal Gravitational Constant
i	inclination
Kn	Knudsen Number
$\bar{l}$	Mean Free Path
L	Characteristic Length
L	Lift Force
m_S	Mass of Satellite
M	Mach Number
M	Mass
M	Mean Anomoly
O	Arbitrary Orbital Element
p	Normal Moentum Flux
$P^m{}_n$	Legendre Function
P_S	Solar Radiation Pressure
r	Radial Vector from Center of Earth to Satellite
r_d	Distance From Geocenter to Third Body
r_s	Vector Towards Sun
R_d	Third Body Disturbing Potential
$\Re$	Gas Constant
S	Cosine of Angle Between Position Vectors of Satellite and Third Body
S	Molecular Speed Ratio
S_{nm}	Gravitational Coefficient
T	Temperature
U	Gravitational Potential Field
U	Velocity
V	Velocity of Satellite

γ	Ratio of Specific Heats
κ	Ellipticity of the Earth
λ	East Longitude of Satellite
μ	Gravitational Constant
ν	Eclipse Factor
ν	Velocity Relative to Atmosphere
θ	Flow Angle
θ	Greenwhich Hour Angle
θ	Solar Panel Angle
ρ	Density
σ	Tangential Momentum Accomadation Coefficient
σ'	Normal Momentum Accomadation Coefficient
τ	Tangential Momentum Flux
ω	Argument of Perigee
Ω	Right Ascention of Ascending Node

Chapter I: Introduction

Space, the so-called final frontier, is beginning to have a tremendous impact on our everyday lives. Satellites in the region of space near the Earth are used for many applications. The impact of communication satellites on our lives is well known and scientific satellites orbiting the Earth are giving us a better understanding of our planet and the Universe. There are plans to launch hundreds of satellites into Low Earth Orbit in the near future. This increased use of the space leads to the need to better understand the environment in which these satellites operate and how that environment interacts with the satellites.

Satellites are put into Low Earth Orbit (LEO) for a number of reasons. Small communication satellites can pass signals back and forth and around the globe more economically than larger satellites in a geostationary orbit. In fact several companies are planning on launching large "constellations" of satellites beginning next year. Earth observation satellites can view the Earth with more detail from lower orbits and the orbit of the satellite can be adjusted to pass over the same spot on the ground at regular intervals. Orbiting observatories, such as the Hubble Space Telescope, are placed in low orbits so they can easily be maintained and retrieved by the Space Shuttle.

One of the problems presented by having so many satellites orbiting the earth is accurately predicting their orbits. Earth observing satellites require their position in orbit to be determined to within centimeters in order to make accurate measurements of the ground below. Owners of communication satellites want their satellites in orbits that are not going to decay too rapidly resulting in the loss of valuable equipment. Predicting the orbit of a satellite would be simple if a point mass satellite was orbiting a point mass Earth in a total vacuum with no other influences. The Earth however, is not a point mass. It's not even a sphere. Other bodies such as the Sun, Moon and planets exert a gravitational influence on the Earth and satellites. Additionally, satellites orbiting as high as 1000 km above the Earth's surface can experience a significant effect on its orbit by the atmosphere. Complicating matters more is that many of the effects are of the same magnitude, making it difficult to distinguish what forces are acting on a satellite.

The effect of the atmosphere on satellites has been studied ever since the first satellite Sputnik I was launched. Because early satellites where often spherical or cylindrical in shape and tumbled through space only the drag force due to the atmosphere was investigated. This was important because the drag force contributes to the decay of the orbit and the effective lifetime of the satellite. Most satellites today however are stabilized in orbit and have large flat solar panels and radar arrays that are fixed in orientation or rotate at regular intervals. These panels can effectively act as wings, producing a lift force and changing the shape of the orbit. Little work has been done to this point to understand the lift effect on satellites.

This project was undertaken to better understand the effect of both aerodynamic lift and drag on Earth orbiting satellites. A new model of the interaction between the atmosphere and the satellite will be applied and a method for predicting the effect of lift on the orbit will be demonstrated. Predictions using this new model will be compared with current methods and areas for improvement will be suggested.

Chapter II: Background

2.1 Free Molecule Flow

Satellites at orbital altitudes experience only a very tenuous atmosphere. This results in a flow regime known as Free Molecule Flow (FMF). The defining characteristic of free molecule flow is that the mean free path traveled by the gas molecules is much larger than the length of the body in the flow. Under these conditions no boundary layer is formed and molecules reemitted from the body do not collide with other molecules until far away from the body. No shock is formed and distortion of the free stream velocity distribution due to the presence of the body can be neglected. In free molecule flow the gas does not behave as a continuous fluid but exhibits some characteristics of its coarse molecular structure (1). One parameter of interest when defining free molecule flow is the Knudsen number (Kn), defined as the ratio of the mean free path of the gas ($\bar{l}$) to a characteristic length (L).

$$Kn = \frac{\bar{l}}{L} \tag{2.1}$$

If Kn>>1 the flow is assumed to be in the free molecule regime.

Since reflected or emitted molecules do not interact with the oncoming flow calculation of the aerodynamic characteristics of a body in free molecule flow can be carried out by considering the flows of incident and reflected or reemitted molecules separately. To do this one must have an understanding of the incoming flow distribution, the interaction between the gas molecules and the surface and the resulting reflected flow distribution.

The incoming flow field is typically assumed to have a uniform velocity profile, superimposed on an equilibrium Maxwellian speed distribution. This is certainly the case if the flow can be said to be hyperthermal. In hyperthermal flow the speed of the body in the flow is much greater than the average random velocity of the gas molecules. The molecular speed ratio (S) can be calculated to determine if a flow can be described as hyperthermal.

$$S = \frac{U}{\sqrt{2\Re T}} = \sqrt{\frac{\gamma}{2}}M \tag{2.2}$$

In the above equation, U is the velocity of the body, T is the temperature of the gas, M is the Mach number of the flow and $\Re$ and γ are gas constants. If the flow is hyperthermal, the Maxwellian velocity distribution of the flow can be ignored but because of the high temperature in the exosphere S if often not that high.

The distribution of reemitted molecules is determined entirely by the interaction of the gas molecules with the surface. If the gas molecules stay in contact with the surface long enough to reach equilibrium with the wall conditions they will be reemitted with no knowledge of their previous velocity. If the molecules are not in contact with the wall long enough to reach equilibrium the distribution of reemitted molecules will retain some knowledge of the incoming flow distribution.

The gas surface interaction (GSI) can adequately be represented by certain average parameters known as accommodation coefficients. Of interest to us are the normal and tangential momentum accommodation coefficients that compare the momentum carried away in the normal and tangential directions to the momentum that would be carried away if the molecule were reemitted diffusely from the wall with a Maxwellian distribution corresponding to the wall temperature T_w, i.e. if the molecules come to complete equilibrium with the wall conditions. Symbolically these coefficients are:

$$\sigma' = \frac{p_i - p_r}{p_i - p_w} \tag{2.3}$$

$$\sigma = \frac{\tau_i - \tau_r}{\tau_i - \tau_w} \tag{2.4}$$

where p and τ are the normal and tangential momentum flux components. The subscripts i and r refer to the incident and reflected fluxes while the subscript w refers to the conditions if the flux was reemitted with a Maxwellian distribution at the wall temperature (1).

There are two hypothetical extreme cases of these two coefficients. Specular reflection refers to the case where the normal momentum of the incoming flow is reversed while the tangential component remains unchanged. For this case $\sigma' = \sigma = 0$. The other extreme case is diffuse remission, where the remitted flux has completely accommodated to the wall temperature T_w and follows a Maxwellian distribution. Then $\sigma' = \sigma = 1$.

Historically, when computing the effect of the atmosphere on satellites the GSI has been assumed to be well known and to result in diffuse reemission (2). This assumption is erroneous, especially if the body has plates presenting a low angle of attack to the oncoming flow (3). Numerous studies have been conducted to determine the momentum accommodation coefficients for a large number of gases, surfaces, and energy levels. A survey of these studies has been conducted by Collins (4,5) resulting the following model for the two momentum accommodation coefficients:

$$\sigma' = 1 - \exp\left[-2.1(\cos\theta)^{1.6}\right] \tag{2.5}$$

$$\begin{aligned} \sigma &= 0.6 - 0.4\left(\frac{45-\theta}{45}\right)^{1.6687} ;\theta \le 45\,\mathrm{deg} \\ \sigma &= 0.6; \theta > 45\,\mathrm{deg} \end{aligned} \tag{2.6}$$

where θ is the angle between the incoming flow and the surface normal as shown in Figure 1.

The normal pressure and shear on a surface element in free molecule flow were shown by Schaaf and Chambre' (1) to be as follows:

$$p = \frac{\rho_\infty U^2}{2S^2}\left[\begin{aligned} &\left(\frac{2-\sigma'}{\sqrt{\pi}} S\sin\theta + \frac{\sigma'}{2}\sqrt{\frac{T_w}{T}}\right)e^{-(S\sin\theta)^2} + \\ &\left\{(2-\sigma')\left[(S\sin\theta)^2 + \frac{1}{2}\right] + \frac{\sigma'}{2}\sqrt{\frac{\pi T_w}{T}}(S\sin\theta)\right\}\left[1 + erf(S\sin\theta)\right] \end{aligned}\right] \tag{2.7}$$

$$\tau = -\frac{\sigma\rho_\infty U^2\cos\theta}{2\sqrt{\pi}}\left\{e^{-(S\sin\theta)^2} + \sqrt{\pi}(S\sin\theta)\left[1 + erf(S\sin\theta)\right]\right\} \tag{2.8}$$

where ρ_∞ is the free stream density, U is the free stream velocity, T_w is the wall temperature, and S is the molecular speed ratio. Equations 2.7 and 2.8 can be integrated over the surface of a body, using a model for the accommodation coefficients, to determine the aerodynamic coefficients C_D and C_L.

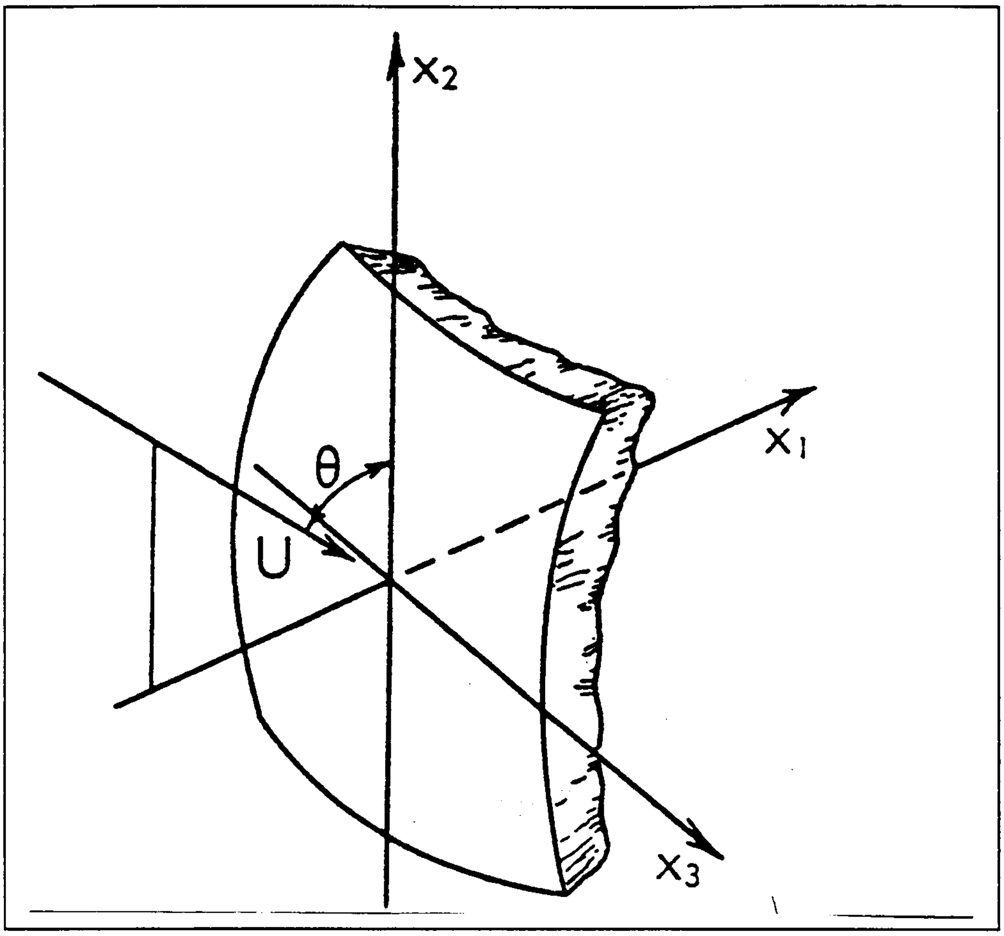

Figure 1. Coordinate System for Gas-Surface Interaction (1)

2.2 Orbit Determination

If the motion of a satellite around a larger body could be completely explained by the two-body problem prediction of that orbit would be very simple. Once the position and velocity of the satellite were know at any one time, Kepler's equations of motion could be applied to find the position of the satellite at any time in the future or the past. In the real world however many other forces effect the motion of a satellite. These other forces are referred to as perturbations and include Earth gravity harmonics, gravitational attraction by the Sun, Moon, and other planets, atmospheric drag, solar radiation pressure, Earth radiation pressure, and ocean and solid Earth tides. In order to accurately predict the orbit of a satellite each of these perturbing forces must be accounted for and modeled.

There are several approaches to solving the equations of motion with perturbations. Most often used are the "special perturbation" techniques. These special perturbation techniques involve the step by step numerical integration of the equations of motion. Two special perturbation techniques are Cowell's method and the Variation of Parameters method.

Cowell's method is the simplest and most straight forward of all the perturbation methods. It was developed in the early 20th century and is especially popular now that computers are becoming faster and more powerful. Cowell's method is to write the equations of motion in the following form:

$$\ddot{\vec{r}} + \frac{\mu}{r^3}\vec{r} = \vec{a}_p \tag{2.9}$$

where $\vec{r}$ is the position vector to the satellite, μ is the gravitational constant of the central body, and $\vec{a}_p$ is the sum of all perturbing accelerations. The main advantage of Cowell's method is its simplicity in formulation and implementation. Some disadvantages include the need for a small integration step when near a large attracting body and the relatively long time needed to integrate the full equations of motion when compared to other methods (6). Despite these shortcomings today's high speed computers make Cowell's method very practical and it is used in several large-scale orbit prediction and determination programs.

The method of variation of parameters has been used since the 1700's and was the only successful perturbation method until the development of modern machine oriented methods such as Cowell's method. A two body orbit can be described by any consistent set of six orbital elements, the most commonly known are Kepler's classical set (a, e, i, ω, Ω, M). The essence of the variation of parameters method is to determine how the set of elements varies with time due to the perturbations. If there where no perturbations the orbital elements would remain constant. Once expressions for the rate of change of the orbital elements are known, they can be numerically integrated to find the values of the elements at some later time. Since the variation in the orbital elements is small compared to the variation in position and velocity, larger integration steps can be taken then with Cowell's method (6).

Satellite orbits are determined from the reduction of tracking data. This tracking data may consist of laser range measurements, visual sighting, radar tracking data, or data from other sources. Tracking data can be entered into a program such as the GEODYN II program to determine the orbit of that satellite. Statistical estimation techniques are used to determine the orbit that best fits that data. This technique requires that several parameters are left as "solved for" parameters (7). The coefficients of drag and radiation pressure are often left as the solved for parameters. This means that these parameters are not entered into the program but are varied by the program until the residuals between the tracking data and the calculated orbit are minimized. These solved-for parameters are able to account for uncertainties in the true coefficients as well as systematic errors in the atmospheric model (8).

2.3 S/HAB Program

The Gentry Supersonic Hypersonic Arbitrary Body Program (S/HABP) (9) is a system of computer routines capable of calculating the supersonic and hypersonic aerodynamic characteristics of arbitrary three-dimensional shapes. The program consists of a geometry generation routine and several aerodynamic routines that apply proven engineering methods to the problem of calculating the aerodynamic characteristics of a body. The program primarily uses local slope pressure techniques. These techniques are most accurate at hypersonic speeds but the first order interference effects of one surface on another can be accounted for to improve accuracy at supersonic speeds (9).

The geometry generation routine in S/HABP uses the surface element or quadrilateral method. Any arbitrary body can be entered as a series of surface points. Sets of four points are grouped together to form a quadrilateral surface element. This surface element is then described by a surface normal vector located at the centroid of the quadrilateral.

The aerodynamic characteristics of a body are calculated in the following manner by the S/HAB program. The pressure at the centroid of each surface element is calculated using a selected pressure calculation method (modified Newtonian, tangent wedge, shock expansion, free-molecule, etc.). This calculated pressure is assumed to be the pressure over the entire surface element. Once the surface pressures are known they can be integrated over the entire body to give the aerodynamic forces and moments.

The pressure calculation method that we are most interested in is the free molecule flow method. When the free molecule flow routine is called the program first determines whether the panel is facing into the flow or away from it. If the panel is facing away from the flow it is said to be in the shadow region and the pressure and shear are assumed to be zero. This is a very accurate assumption if the speed ratio is large i.e., if the flow is hyperthermal. If the panel is facing into the flow the pressure and shear are calculated using the formulas given by Schaaf and Chambre (Equations 2.6 and 2.7) (9).

The program accepts the momentum accommodation coefficients as input variables and treats them as constants. It is a simple matter however to modify the program to use accommodation coefficients that vary with the relative flow angle such as equations 2.4 and 2.5. Other parameters that must be entered into the program are the free stream temperature and pressure, and the Mach number of the flow.

2.4 GEODYN II Program

The GEODYN II program was developed at the NASA/Goddard Space Flight Center for the purpose of satellite orbit determination, geodetic parameter estimation, and many other items relating to satellite geodesy. The GEODYN II program operates in two main modes, an orbit generation mode using Cowell's method of integrating the orbit, and a data reduction mode using a Bayesian least squares statistical estimation procedure (8).

We are primarily interested in the orbit generation mode of the GEODYN II program. This mode uses the direct numerical integration outlined in Cowell's method. The GEODYN II program models the following perturbation accelerations: nonspherical Earth harmonics, luni-solar potentials, planetary potential, radiation pressure, solid Earth and ocean tidal potential, atmospheric drag, and general accelerations. The models of each of these forces will be briefly discussed below. The equation of motion used by the GEODYN program is of a slightly different form than Equation 2.9. If terms are regrouped and it is recognized that gravitational attractions can be described by a potential field the equation of motion can be written as

$$\ddot{\vec{r}} = \nabla U + \vec{A}_D + \vec{A}_R \tag{2.10}$$

where U is the potential field due to gravity and $\vec{A}_D$ and $\vec{A}_R$ are the accelerations due to drag and solar radiation pressure respectively.

The Earth's Gravity field is expressed by the potential of an ellipsoid of revolution and small irregular variations expressed as a sum of spherical harmonics. The GEODYN system uses this formulation:

$$U = \frac{GM}{r}\left[1 + \sum_{n=2}^{n\max}\sum_{m=0}^{n}\left[\frac{a_e}{r}\right]^n P_n^m(\sin\phi')\left[C_{nm}\cos m\lambda + S_{nm}\sin m\lambda\right]\right] \tag{2.11}$$

where G is the universal gravitational constant, M is the mass of the Earth, r is the distance to the satellite, n max is the summation limit, a_e is the Earth's mean equatorial radius, ϕ' is the satellites geocentric latitude, λ is the satellites east longitude, P_n^m (sin ϕ') indicates the associated Legendre function, and C_{nm} and S_{nm} are the denormalized gravitational coefficients.

Perturbations due to a third body are treated by defining a third body disturbing potential R_d. This potential is of the form

$$R_d = \frac{Gm_d}{r_d}\left[\left[1-\frac{2r}{r_d}S+\frac{r^2}{r_d^2}\right]^{-\frac{1}{2}} - \frac{r}{r_d S}\right] \tag{2.12}$$

where m_d is the mass of the disturbing body, r_d is the distance from the geocenter to the disturbing body, and S is the cosine of the angle between the position vectors of the satellite and disturbing body.

The GEODYN system incorporates several methods for calculating the perturbation due to solid Earth and ocean tides. Most result in spherical harmonic variations in the gravitational potential similar in form to Equation 2.10. A complete description can be found in the GEODYN II Systems Description (10).

The GEODYN program can account for the force due to the radiation pressure for radiation directly from the sun and reflected off the Earth. The acceleration due to solar radiation takes the form

$$\vec{A}_R = -\nu C_R \frac{A_s}{m_s} P_s \hat{r}_s \tag{2.13}$$

where ν is the eclipse factor, C_R is the coefficient of reflectivity, A_s is the cross sectional area of the satellite, m_s is the mass of the satellite, P_s is the solar radiation pressure in the vicinity of the Earth and $\hat{r}_s$ is true of date unit vector pointing towards the Sun. The acceleration due to the radiation reflected by the Earth is modeled in a similar manner with the Earth represented by 19 reflecting surfaces.

The acceleration due to atmospheric drag is of the form

$$\vec{A}_D = -\frac{1}{2} C_D \frac{A_s}{m_s} \rho v \vec{v} \tag{2.14}$$

where C_D is the drag coefficient, ρ is the density of the atmosphere at the satellite position, and v is the velocity of the satellite relative to the atmosphere. The GEODYN program uses the Jacchia 71 model to calculate the density of the atmosphere. This model is the most accurate available and accounts for the effects of solar activity, geomagnetic activity, and diurnal, latitudinal and seasonal variations in the upper atmosphere. The rotation of the upper atmosphere is also accounted for when calculating the drag force (10).

2.5 The ERS-1 Satellite

The first European Remote Sensing Satellite (ERS-1) was launched to increase our understanding of the interaction between the Earth's atmosphere and oceans in order to improve global climate modeling. It was launched into a Sun-synchronous polar orbit allowing it to view the entire Earth as it rotates beneath it. The Sun-synchronous orbit is designed so that the orbital plane will always maintain its position relative to the sun. This is beneficial in that the solar array only needs to rotate about one axis normal to the orbital plane. ERS-1 is able to change its orbit slightly to vary the repeat period of its ground track.

The primary instruments on ERS-1 are a number of microwave radars used for measuring surface and wave heights, a radar altimeter, and a passive Laser Retro-Reflector used as a target by ground-based laser tracking stations. The ERS-1 Satellite as depicted in Figure 2 consists of a prismatic payload section measuring approximately 2 m x 2 m x3 m, a large solar array measuring 12 m x 2.4 m which is free to rotate a full 360° over the course of one orbit, and several radar antennas (11).

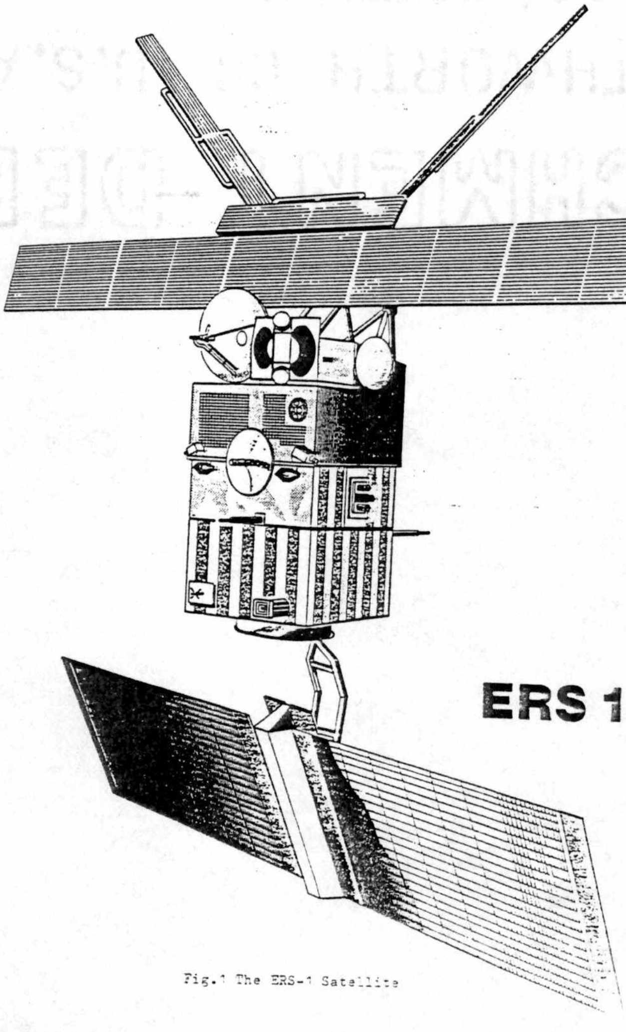

Figure 2. The ERS-1 Satellite (12)

Chapter III: Methodology

3.1 Aerodynamic Modeling of ERS-1

The first step in understanding the effect of aerodynamics on a satellite's orbit is to develop a model of the aerodynamic characteristics of the satellite. This task is easily

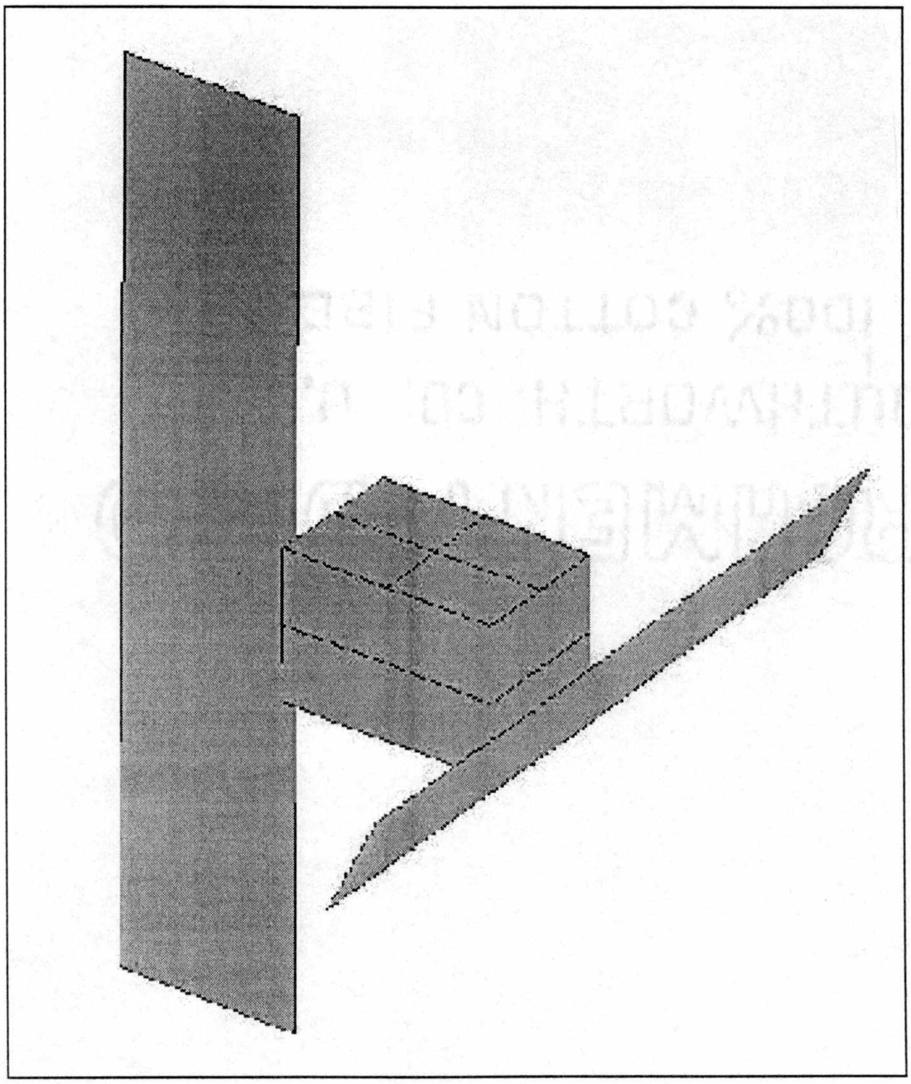

Figure 3. Geometric Model of ERS-1

performed using the S/HAB program.

The relatively simple geometry of the ERS-1 satellite can easily be represented by a number of flat plates. The satellite consists of three sections, the payload and support structure, the solar panel, and the radar antenna. Figure 3 shows the geometric representation of the satellite as entered into the S/HAB program. The body of the satellite is 2 m x 2 m x 3 m, the solar panel is 12 m x 2.5 m, and the radar antenna is 1 m x 10 m. The solar panel and radar antenna are modeled having both a front and a back side; this is important so that all the shear force can be accounted for. Several geometries have been developed, each representing the solar panel in a different position as it rotates about the y-axis of the satellite. Since the satellite is stabilized in orbit, only the solar panel changes position relative to the oncoming flow.

The free molecule flow routine of the S/HAB program was used to calculate the lift and drag coefficients of the satellite. Two cases were run, first the diffuse case where $\sigma=\sigma'=1$, and the second case where σ and σ' vary with the incoming flow angle.

Parameters that have to be entered into the S/HAB program are the ratio of the satellite wall temperature to the free stream temperature, the free stream Mach number, the altitude, and the cross-sectional area of the satellite. The ratio of wall temperature to free stream temperature varies depending on the solar heating of the satellite and the atmosphere, magnetic activity, time of day, and the position of the satellite above the Earth. For the purpose of our analysis, it was assumed that the satellite had an average wall temperature of 300 K and the free stream temperature averaged 850 K during the period of interest from May to December 1993. The free stream Mach number was entered as 6.3 (S=5.3) based on this same temperature and the velocity of a satellite in a near circular orbit 780 km above the Earth. The altitude of the satellite was entered as 780 km and the nominal cross sectional area of the satellite is 36 m^2 when the solar panel is perpendicular to the flow.

3.2 Conversion of Orbital Data from IERS to ECI

A set of position and velocity vectors has been provided for the ERS-1 satellite by Dr. B.E. Schutz at the University of Texas Center for Space Research. A position and velocity vector is given every three and a half day for the period from May 31, 1993, till December 17, 1993. This set of orbital data was created from laser ranging data using a program similar to the GEODYN II program. These orbits represent a best fit of the current perturbation models to the laser tracking data for an arc length of 3.5 days. There may be discontinuities of 10-20 cm between adjacent arcs but the first point in the arc is the most accurate prediction of the satellites position available. In the reduction of the tracking data, the drag coefficient and the coefficient of reflectivity are the solved-for parameters. These parameters are treated as constants and adjusted once a day to produce an accurate orbit.

The data provided was referenced in the International Earth Rotating System (IERS), a rotating coordinate frame. This fact leads to the need to convert the data to an Earth Centered Inertial (ECI) or True of Date (TOD) coordinate system for entry into the GEODYN Program and for analysis. To perform this transformation the IERS coordinate frame simply must be rotated about the z-axis through the Greenwich angle. The following equations are used to rotate the coordinate frame:

$$X_i = X_e \cos\theta - Y_e \sin\theta \tag{3.1}$$

$$Y_i = X_e \sin\theta + Y_e \cos\theta \tag{3.2}$$

$$\dot{X}_i = \dot{X}_e \cos\theta - \dot{Y}_e \sin\theta \tag{3.3}$$

$$\dot{Y}_i = \dot{X}_e \sin\theta + \dot{Y}_e \cos\theta \tag{3.4}$$

where θ is the Greenwich angle, ω_e is the angular velocity of the Earth, and the subscripts i and e represent the inertial and Earth centered frames respectively. The Greenwich angle is obtained from the Astronomical Almanac. Once the observations have been converted to ECI they can readily be entered into the GEODYN program and the corresponding orbital elements obtained.

3.3 Development of Baseline Orbit and Separation of Drag Perturbation

While the data provided by UTCSR provides a set of initial positions for our comparison of perturbation models, a more complete baseline orbit is need to conduct our analysis. This baseline orbit can be developed using the GEODYN II program. Each data point provided can be entered as a starting point for the GEODYN orbit prediction routine. The most current perturbation models incorporated into the program will be used to project the orbit forward until the next data point is reached. Since the baseline orbit will represent a typical orbit prediction the Drag Coefficient will be taken as a constant of 2.0. This value is the limit for diffuse scattering on a sphere as $S \rightarrow \infty$, and has historically been used for the prediciton of satellite orbits. The coefficient of reflectivity will be taken as 0.083 which is the average of solar panel with a reflectivity of 0.0 and the satellite body with a reflectivity of 0.5. These reflectivity values were provided by UTCSR.

The actual orbit of a satellite can be represented by a Keplerian orbit and a sum of perturbating effects, such as atmpospheric drag, non-spherical harmonics, and third body effects.

$$O_{actual} = O_{kepler} + \sum \Delta O_i \tag{3.5}$$

This fact will allow us to separate the effect of aerodynamic forces from the rest of the orbit. The GEODYN program can be used to create an orbit that accounts for the Keplerian orbit as well as all perturbations except the drag perturbation. This orbit can then be subtracted from the baseline orbit leaving the perturbation due to aerodynamic forces.

$$\Delta O_{AF} = O_{Baseline} - O_{NoDrag} \tag{3.6}$$

This is possible since any of the pertubations on the orbit are small when compared to the Keplerian orbit and their influence on each other can be neglected. The perturbation due to the aerodynamic forces can then be compared to the perturbation predicted by our new model using the technique outlined in the next section.

3.4 Calculation of the Aerodynamic Perturbation

A variation of parameters approach can be taken to determine the aerodynamic perturbation on a satellite orbit. This technique has been used by both Moore and Sowter (13) and Crowther and Stark (14) to analyze the orbit of the Astronomical Netherlands

Satellite (ANS-1). Their approach was to separate the forces acting on the satellite into components acting along the satellite's track, radially from the center of the Earth to the satellite, and perpendicular to the orbital plane. These force components can be substituted into Lagrange's planetary equations, relating the change in semi-major axis (a), eccentricity (e), and inclination (i) to the change in the eccentric anomaly (E).

$$\frac{da}{dE} = \frac{2ra^2V}{\mu}\sqrt{\frac{a}{\mu}}F_t \tag{3.7}$$

$$\frac{de}{dE} = \frac{r}{V}\sqrt{\frac{a}{\mu}\left\{2F_t\left[e + \frac{a}{r}(\cos E - e)\right] + F_r\sqrt{1-e^2}\sin E\right\}} \tag{3.8}$$

$$\frac{di}{dE} = \frac{ar}{\mu\sqrt{1-e^e}}\left\{\cos\omega\cos E - \sqrt{1-e^2}\sin\omega\sin E - e\cos\omega\right\}F_n \tag{3.9}$$

In the above equations r is the distance from the center of the Earth to the satellite, V is the satellite's velocity, μ is the gravitation constant for the Earth, ω is the argument of perigee, and F_r, F_t, and F_n are the forces acting in the radial, tangential, and normal directions. Crowther and Stark (14) used this approach to derive values for the momentum accommodation coefficients from analysis of the change in semi-major axis and inclination. Moore and Sowter (13) derived values of the momentum accommodation coefficients from analysis of the semi-major axis , eccentricity, and inclination. Both these studies were limited by the accuracy of the available satellite ephemeris.

Our analysis is simplified by the fact that since the ERS-1 is stabilized in its orbit the drag force acts only in the tangential direction, and the lift force acts only in the normal direction.

$$F_r = L = \frac{1}{2} C_L \rho V^2 \tag{3.11}$$

$$F_t = D = -\frac{1}{2} C_D \rho V^2 \tag{3.12}$$

$$F_n = 0 \tag{3.13}$$

Since no aerodynamic force acts in the direction normal to the orbit we are left with two equations describing the change in the orbit. The radial position of a satellite in an orbit and its velocity at that point can be related to the orbital parameters by the following equations (6).

$$r = a(1 - e\cos E) \tag{3.14}$$

$$V^2 = \frac{\mu}{a\left(1 - e^2\right)} \frac{1 + e\cos E}{1 - e\cos E} \tag{3.15}$$

This results in two equations for the variation of two orbital parameters that depend only on the eccentric anomaly and the density of the atmosphere. These two equations can be integrated over one orbit resulting in the incremental change in that orbital element over one orbital period (13).

$$\Delta a = \int_0^{2\pi} \frac{da}{dE} dE \tag{3.16}$$

$$\Delta e = \int_0^{2\pi} \frac{de}{dE} dE \tag{3.17}$$

One of the more uncertain elements in any analysis of satellite orbits is the value of the free stream density at any point. The most accurate model of the upper atmosphere available is the Jacchia 71 model. This model accounts for solar and magnetic flux effects, the time of day, seasonal and latitudinal variations and several other factors and is based on a large number of empirical measurements (15). Implementation of this model is rather cumbersome requiring tables of solar and magnetic flux values on the day of interest, the solar ephemeris, and temperature variations due to latitude and time of day. Since the variational changes in density over time are better understood and modeled than the absolute density, a simpler model to implement has been developed by King-Hele (16). In this model the well-understood variations due to position and height in an oblate atmosphere are referenced to the density at the perigee point of the orbit.

$$\rho = \rho_p k_1 e^{z \cos E}\left[1 + c\cos 2(\omega + E) - 2ce\sin 2(\omega + E)\sin E + \frac{1}{4}c^2\{1 + \cos 4(\omega + E)\}\right] \tag{3.18}$$

$$k_1 = e^{-z-c\cos 2\omega} \tag{3.19}$$

$$c = \frac{1}{2}\frac{r_p \kappa}{H}\sin^2 i \tag{3.20}$$

$$z = \frac{ae}{H} \tag{3.21}$$

In the above equations ρ_p is the density at perigee, H is the atmospheric scale height, and κ is the ellipticity of the Earth. Both the density at perigee and the scale height can be obtained from the 1966 supplement to the U.S. Standard Atmosphere (17).

Chapter IV: Results

4.1 Aerodynamic Model

The aerodynamic characteristics of the ERS-1 satellite were modeled using the Supersonic/Hypersonic Arbitrary Body Program. Two models were developed. The first calculated lift and drag coefficients using the diffuse model for reemission. The second used momentum accommodation coefficients that varied with the angle of the incoming flow. Both models were created for a wall to free stream temperature ratio of 0.35 and a molecular speed ratio of 5.27 (M=6.3) (Figures 4 and 5).

Figure 4 shows the drag coefficient calculated versus the angle of the satellite's solar panel. Since the satellite is stabilized in orbit so that the radar arrays are always parallel to the Earth, the solar panel is the only component that changes orientation relative to the oncoming flow. It is interesting to note that the variable model predicts lower drag at small angles to the incoming flow but at high angles it predicts significantly more drag. Curves were fit to both sets of data for use in the orbital perturbation program. These curves are as follows:

$$C_{Ddiffuse} = 1.22308 + 2.58572\sin(\theta) + 0.925154\sin(\theta)^2 \tag{4.1}$$

$$C_{D\,variable} = 1.11743 + 1.26263\sin(\theta) + 2.65699\sin(\theta)^2 \tag{4.2}$$

where θ is the solar panel angle in degrees.

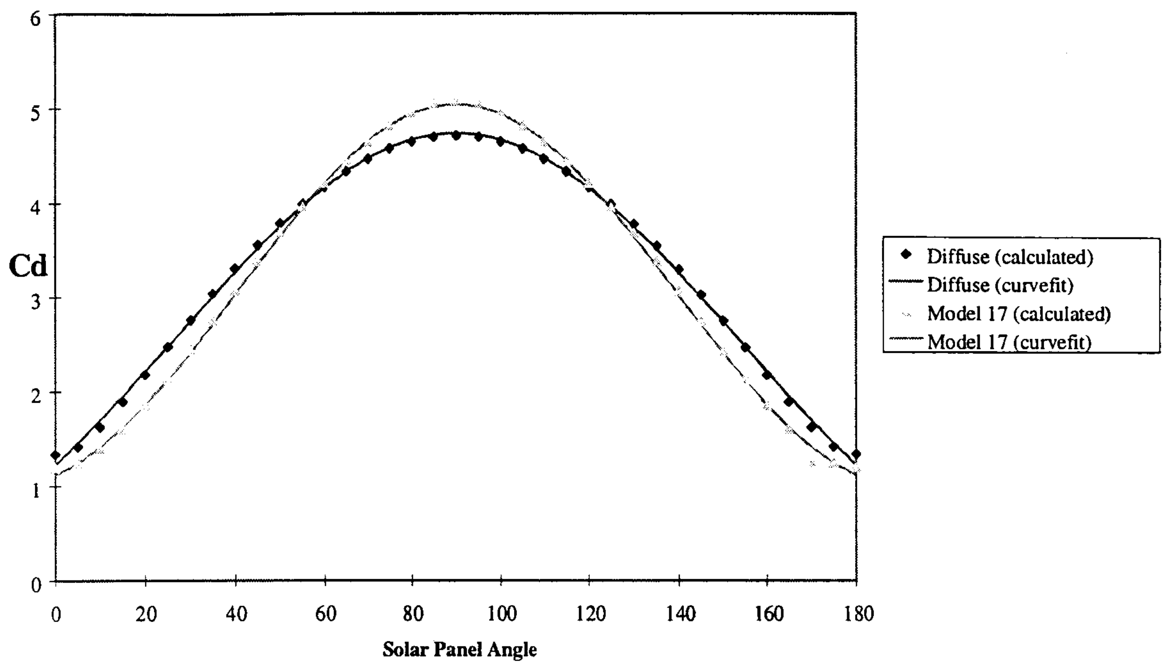

Figure 4. Coefficient of Drag

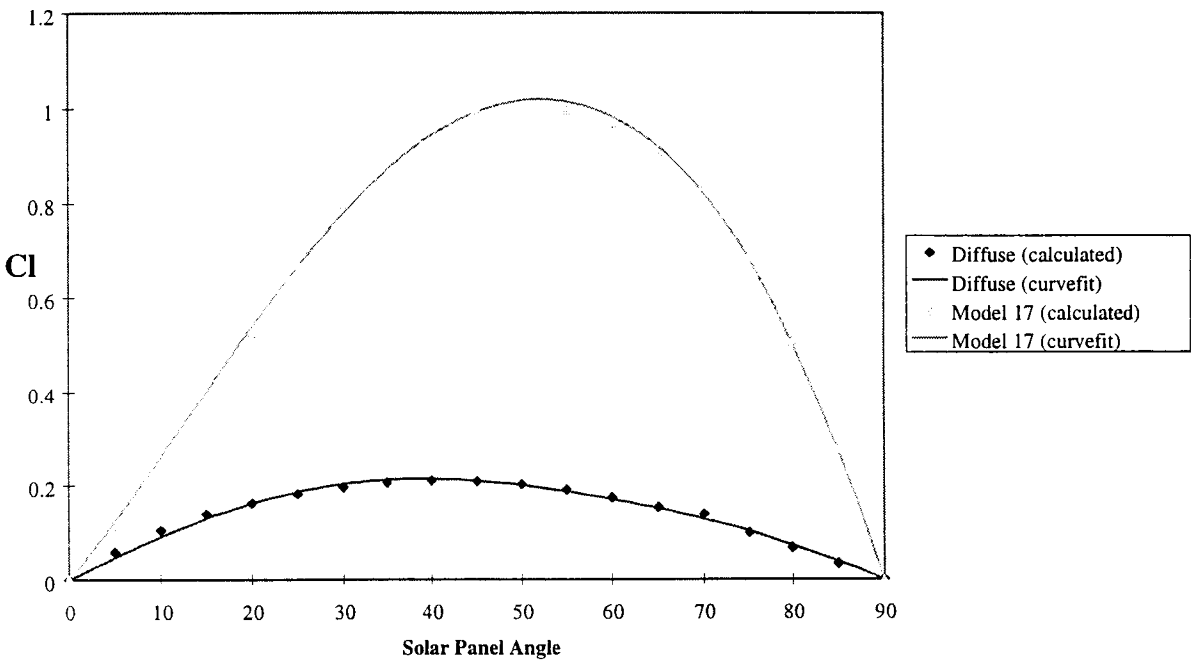

Figure 5. Coefficient of Lift

The lift coefficient versus solar panel angle is shown in Figure 5. It is immediately obvious that the variable model predicts much more lift than the diffuse model. It can also be noted that the peak lift shifts from about 35 degrees for the diffuse case to about 50 degrees for the variable case. The following curves were fit to the lift data for use in the orbital perturbation program.

$$C_{Ldiffuse} = 0.272403\sin\left(\frac{\theta}{2}\right) - 0.000402033\theta\sin\left(\frac{\theta}{2}\right) - 0.00997102\theta\sin\left(\frac{\theta}{2}\right)^2 \qquad (4.3)$$

$$C_{L\,variable} = 0.658977\sin\left(\frac{\theta}{2}\right) + 0.0114795\theta\sin\left(\frac{\theta}{2}\right) - 0.00406447\theta\sin\left(\frac{\theta}{2}\right)^2 \qquad (4.4)$$

4.2 Conversion of Orbital Data

The orbital data provided by the Center for Space Research at the University of Texas required conversion from the International Earth Rotating System (IERS) to an Earth Centered Inertial (ECI) coordinate system. This conversion simply required a rotation of the IERS frame about the Z-axis. This rotation was performed by the computer program entitled THETA found in Appendix A.

4.3 Calculation of the Aerodynamic Perturbation

The calculation of the orbital perturbation due to aerodynamic effects was calculated using the approach detailed in section 3.4. This calculation was performed by the PERT program listed in Appendix A. The PERT program uses a fourth order Runge-Kutta integrator to calculate the perturbation in the semi-major axis and the eccentricity over one orbit. All parameters (A, e, ρ_0, i, H) are assumed constant over one orbit and the

initial orbital elements are based on a GEODYN orbit produced with a drag coefficient of 0.0. Figure 6 shows the progression of the semi-major axis and eccentricity of the No Drag orbit over the course of a typical 3.5 day arc.

The calculated perturbation in the semi-major axis is shown in Figure 7. The first thing to note is that the variable model predicts a larger perturbation than the diffuse case. Also note that the calculated perturbation is relatively constant in each of the cases shown. However, the GEODYN calculation shows tremendous variability and irregularity. The different density models used in the GEODYN and PERT programs could account for the differences between the two predictions. This effect will be examined later.

The calculated perturbation in eccentricity is shown in Figure 8. It is interesting to note that the trends predicted by both the GEODYN and PERT programs show more correlation for the eccentricity than they did for the semi-major axis. Magnitude differences still exist, again probably relating to the different density models used in each program.

The choice of atmospheric model and parameters plays a vital role in the prediction of aerodynamic perturbations. Figure 9 shows the variation in predicted perturbations using the variable coeffiecient model with different free stream temperatures and therefore different perigee densities entered into the PERT program. It is obvious that the density model can have a large effect on the calculated perturbations. The GEODYN program uses the Jacchia 71 atmospheric model which can account for small scale and day to day variations in the density at a given point. The exponentially varying oblate atmosphere

initial orbital elements are based on a GEODYN orbit produced with a drag coefficient of 0.0. Figure 6 shows the progression of the semi-major axis and eccentricity of the No Drag orbit over the course of a typical 3.5 day arc.

The calculated perturbation in the semi-major axis is shown in Figure 7. The first thing to note is that the variable model predicts a larger perturbation than the diffuse case. Also note that the calculated perturbation is relatively constant in each of the cases shown. However, the GEODYN calculation shows tremendous variability and irregularity. The different density models used in the GEODYN and PERT programs could account for the differences between the two predictions. This effect will be examined later.

The calculated perturbation in eccentricity is shown in Figure 8. It is interesting to note that the trends predicted by both the GEODYN and PERT programs show more correlation for the eccentricity than they did for the semi-major axis. Magnitude differences still exist, again probably relating to the different density models used in each program.

The choice of atmospheric model and parameters plays a vital role in the prediction of aerodynamic perturbations. Figure 9 shows the variation in predicted perturbations using the variable coeffiecient model with different free stream temperatures and therefore different perigee densities entered into the PERT program. It is obvious that the density model can have a large effect on the calculated perturbations. The GEODYN program uses the Jacchia 71 atmospheric model which can account for small scale and day to day variations in the density at a given point. The exponentially varying oblate atmosphere

initial orbital elements are based on a GEODYN orbit produced with a drag coefficient of 0.0. Figure 6 shows the progression of the semi-major axis and eccentricity of the No Drag orbit over the course of a typical 3.5 day arc.

The calculated perturbation in the semi-major axis is shown in Figure 7. The first thing to note is that the variable model predicts a larger perturbation than the diffuse case. Also note that the calculated perturbation is relatively constant in each of the cases shown. However, the GEODYN calculation shows tremendous variability and irregularity. The different density models used in the GEODYN and PERT programs could account for the differences between the two predictions. This effect will be examined later.

The calculated perturbation in eccentricity is shown in Figure 8. It is interesting to note that the trends predicted by both the GEODYN and PERT programs show more correlation for the eccentricity than they did for the semi-major axis. Magnitude differences still exist, again probably relating to the different density models used in each program.

The choice of atmospheric model and parameters plays a vital role in the prediction of aerodynamic perturbations. Figure 9 shows the variation in predicted perturbations using the variable coeffiecient model with different free stream temperatures and therefore different perigee densities entered into the PERT program. It is obvious that the density model can have a large effect on the calculated perturbations. The GEODYN program uses the Jacchia 71 atmospheric model which can account for small scale and day to day variations in the density at a given point. The exponentially varying oblate atmosphere

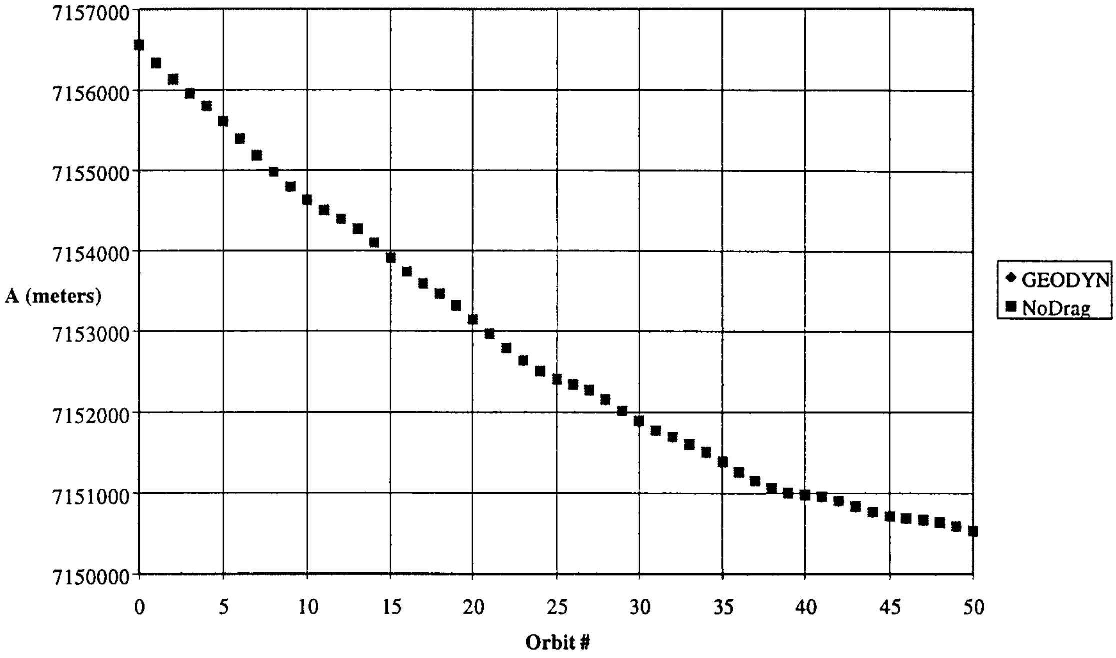

(a) Semimajor Axis

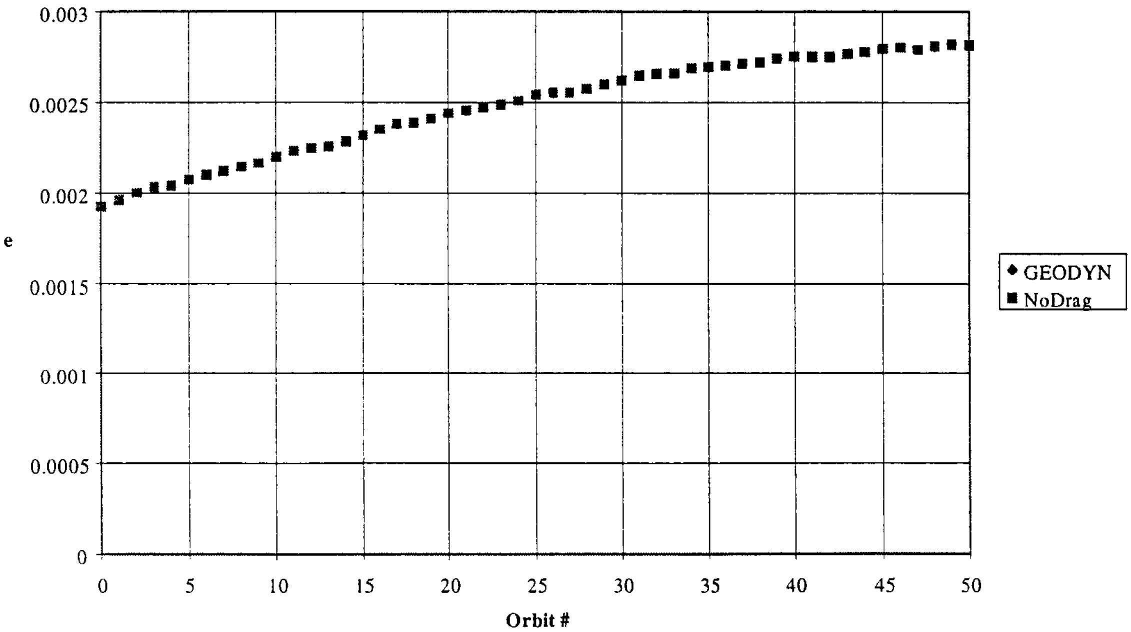

(b) Eccentricity

Figure 6. Progression of Orbital Elements

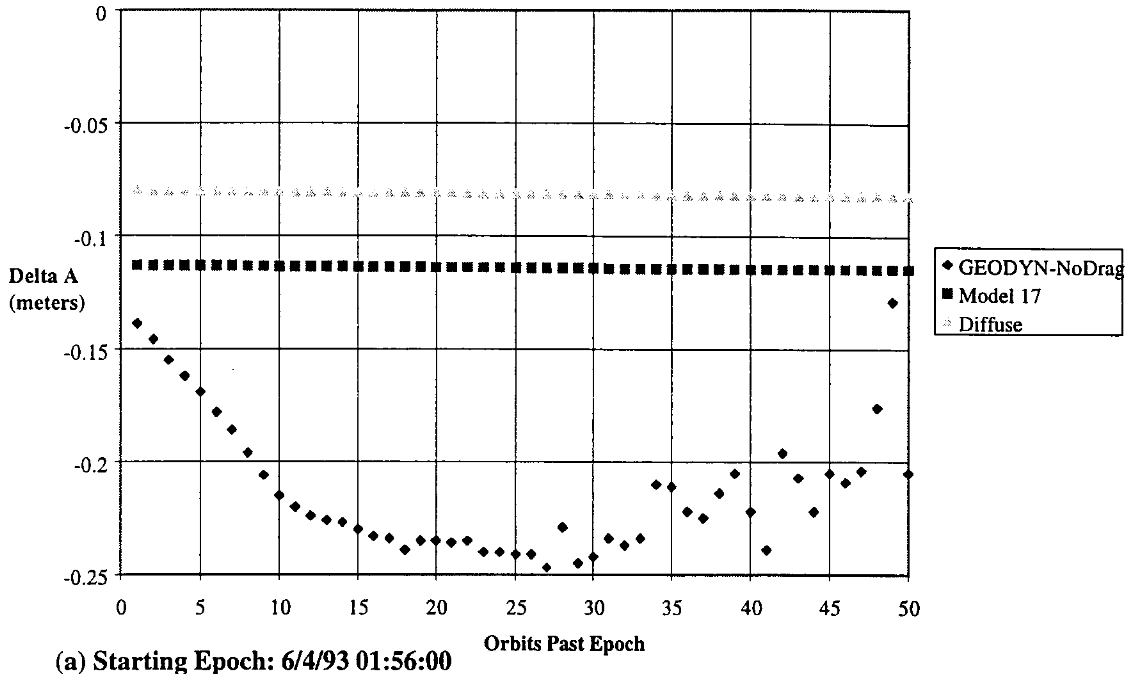

(a) Starting Epoch: 6/4/93 01:56:00

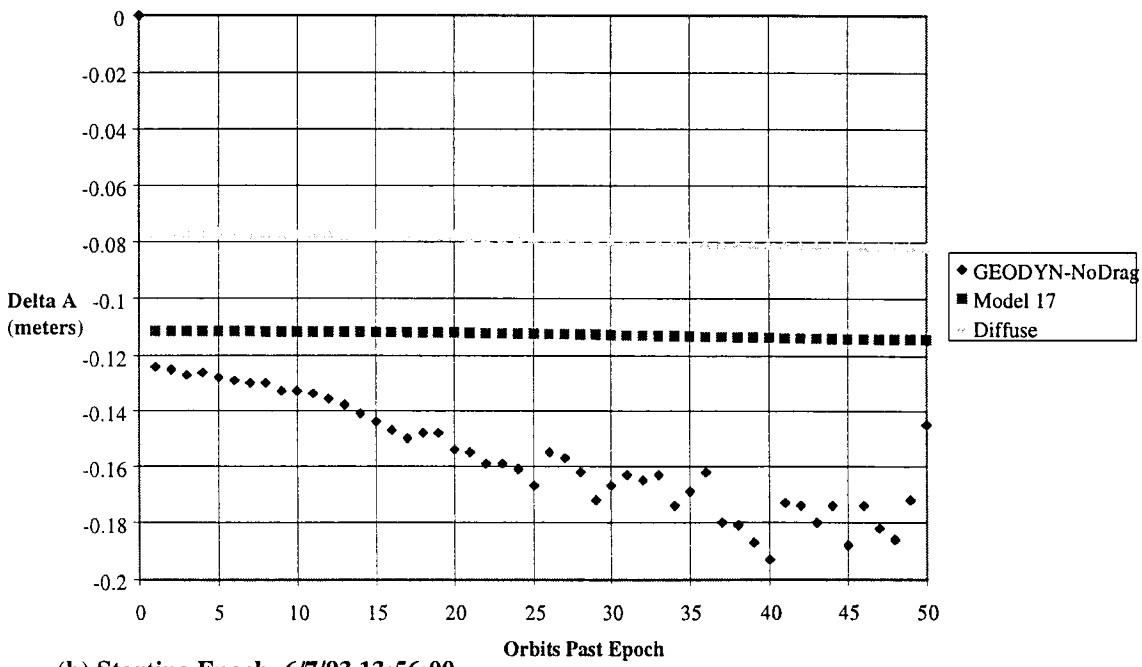

(b) Starting Epoch: 6/7/93 13:56:00

Figure 7. Change in Semi-Major Axis

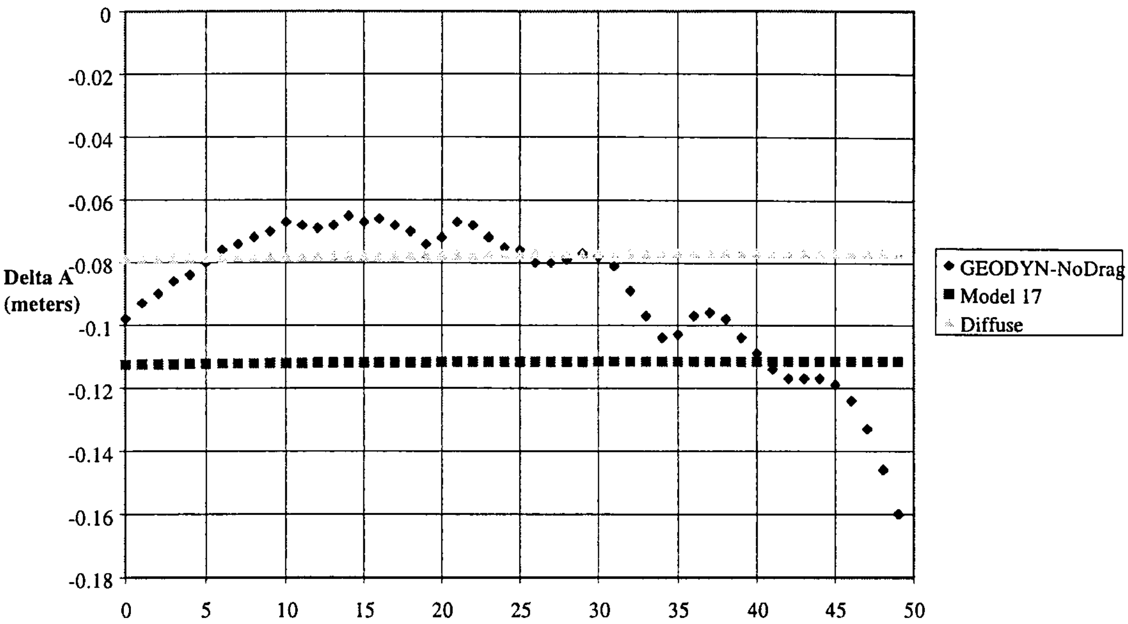

(c) Starting Epoch: 6/11/93 01:56:00

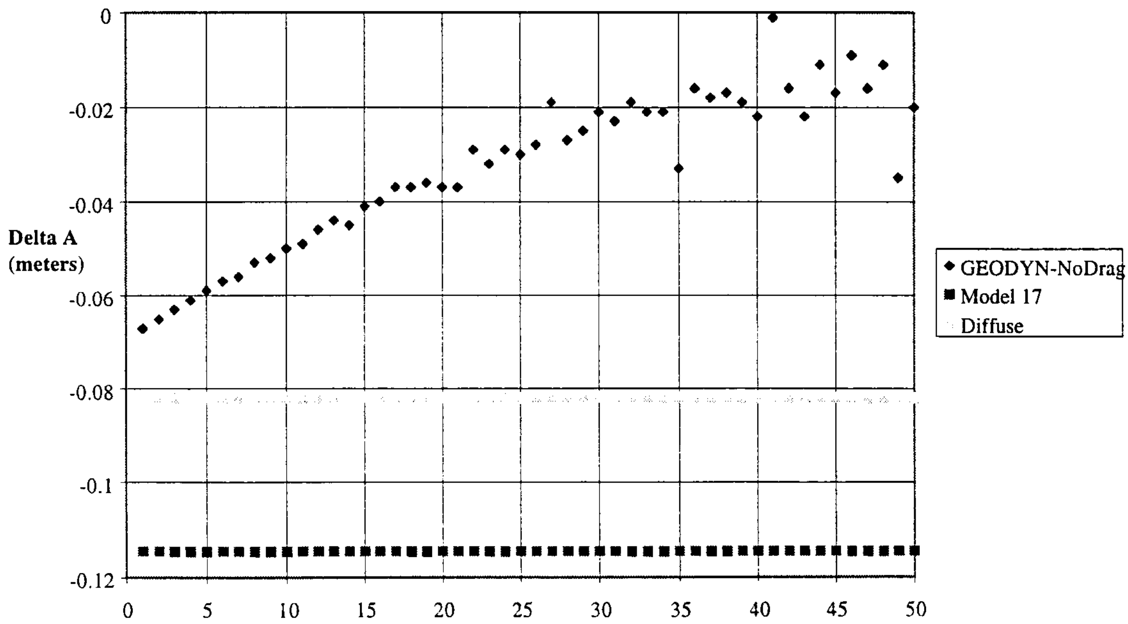

(d) Starting Epoch: 6/14/93 13:56:00

Figure 7. Change in Semi-Major Axis (continued)

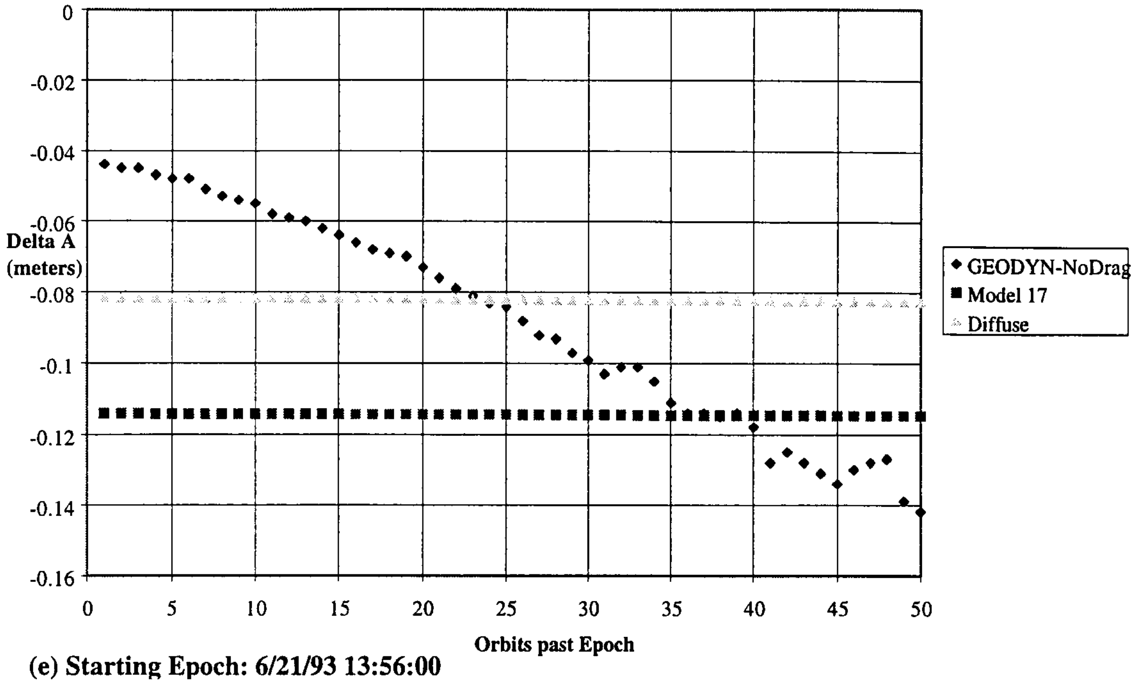

(e) Starting Epoch: 6/21/93 13:56:00

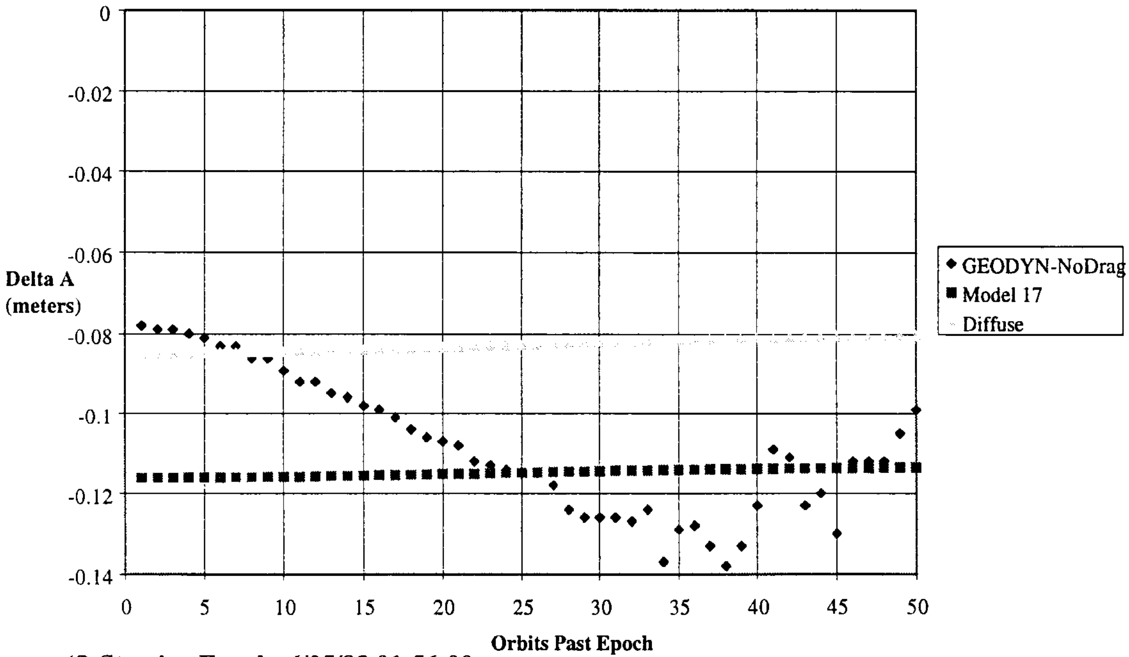

(f) Starting Epoch: 6/25/93 01:56:00

Figure 7. Change in Semi-Major Axis (continued)

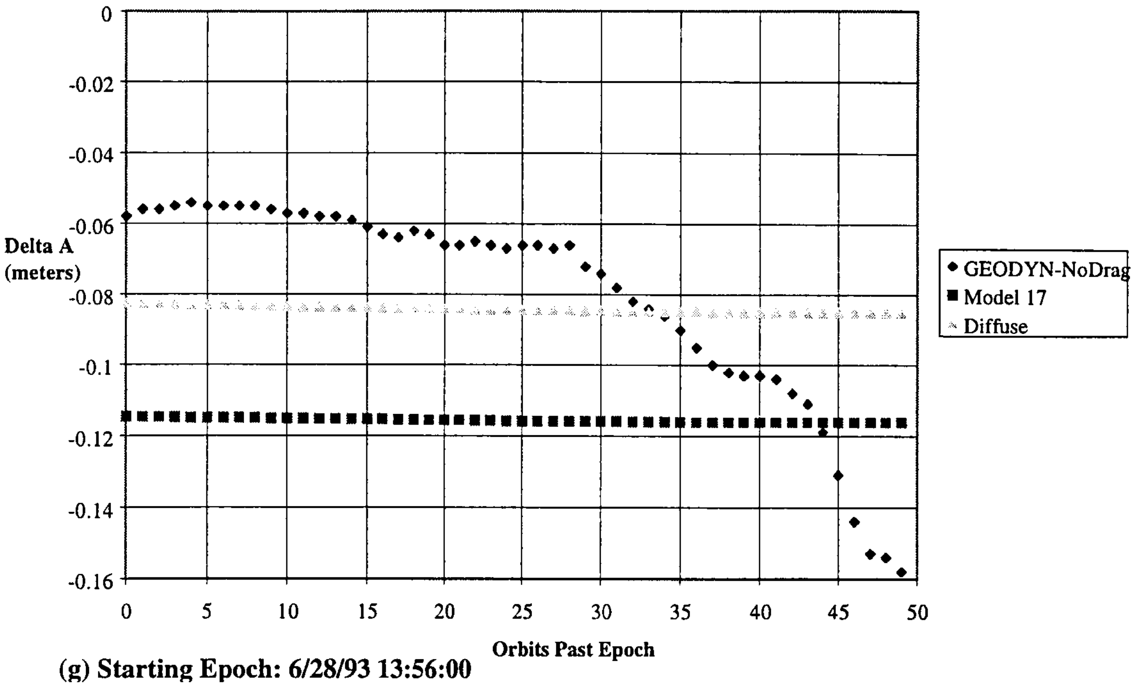

(g) Starting Epoch: 6/28/93 13:56:00

Figure 7. Change in Semi-Major Axis (continued)

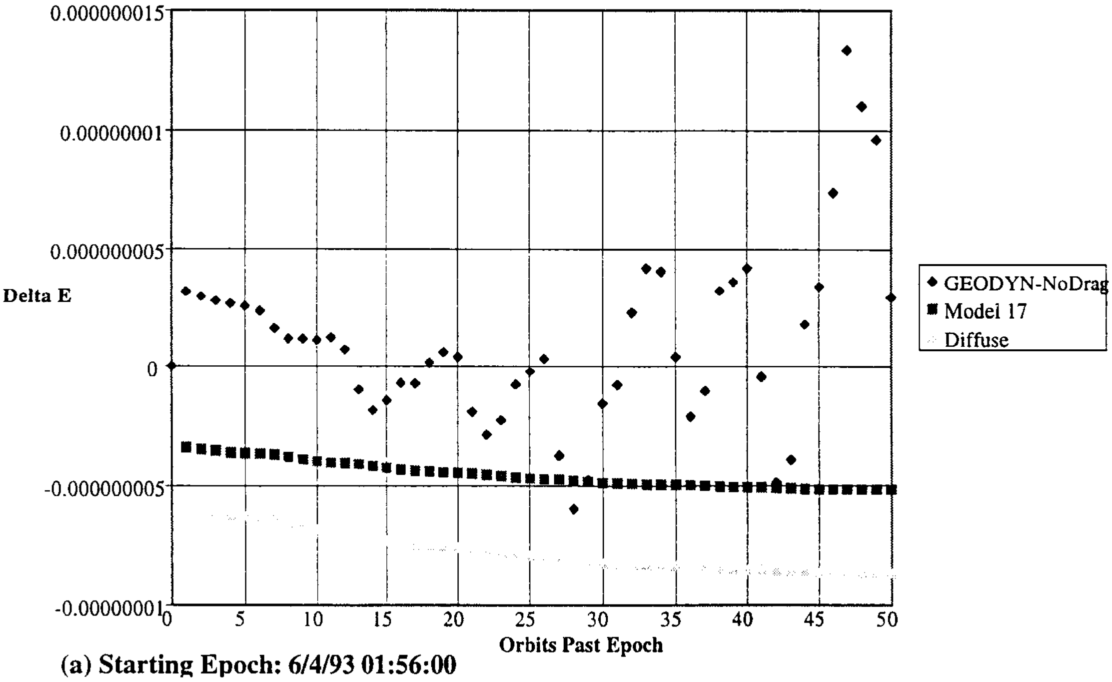

(a) Starting Epoch: 6/4/93 01:56:00

Figure 8. Change in Eccentricity

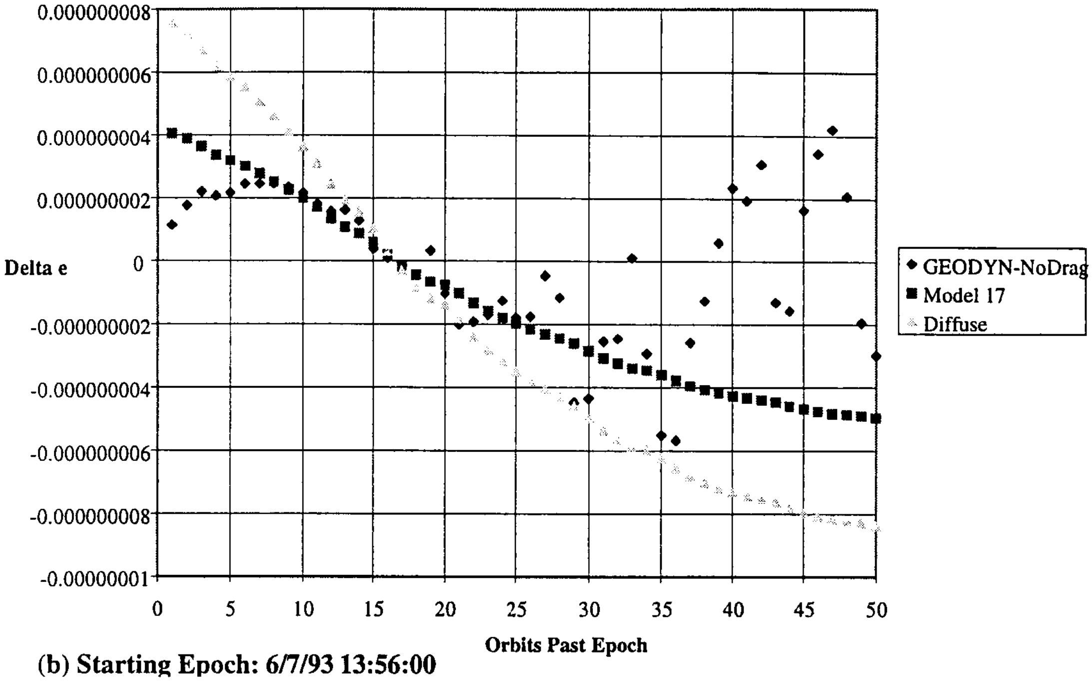

(b) Starting Epoch: 6/7/93 13:56:00

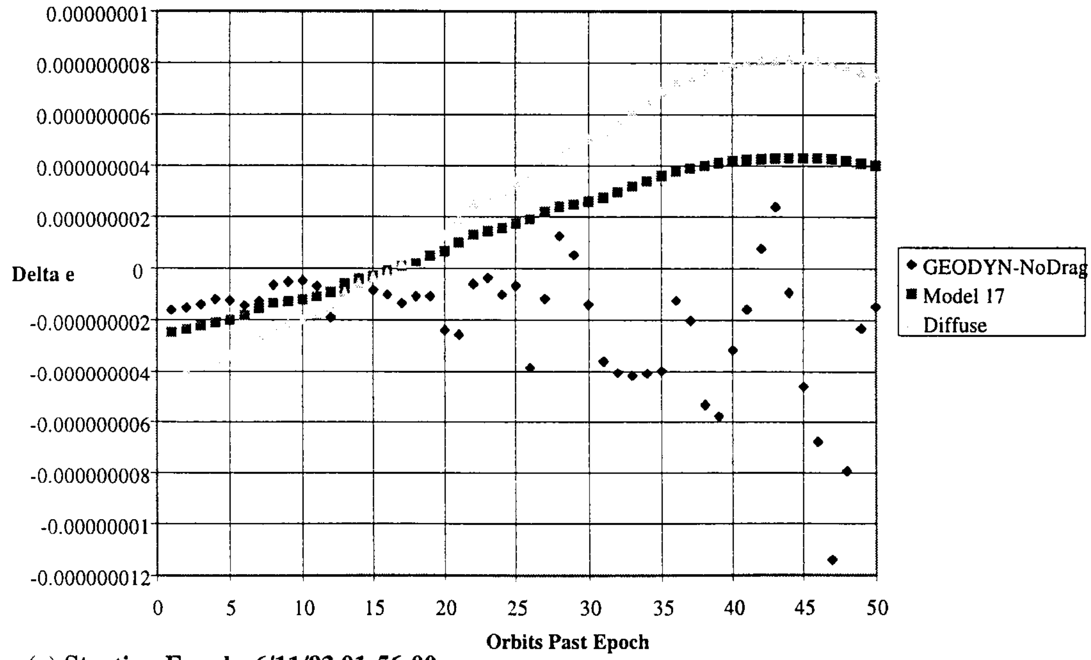

(c) Starting Epoch: 6/11/93 01:56:00

Figure 8. Change in Eccentricity (continued)

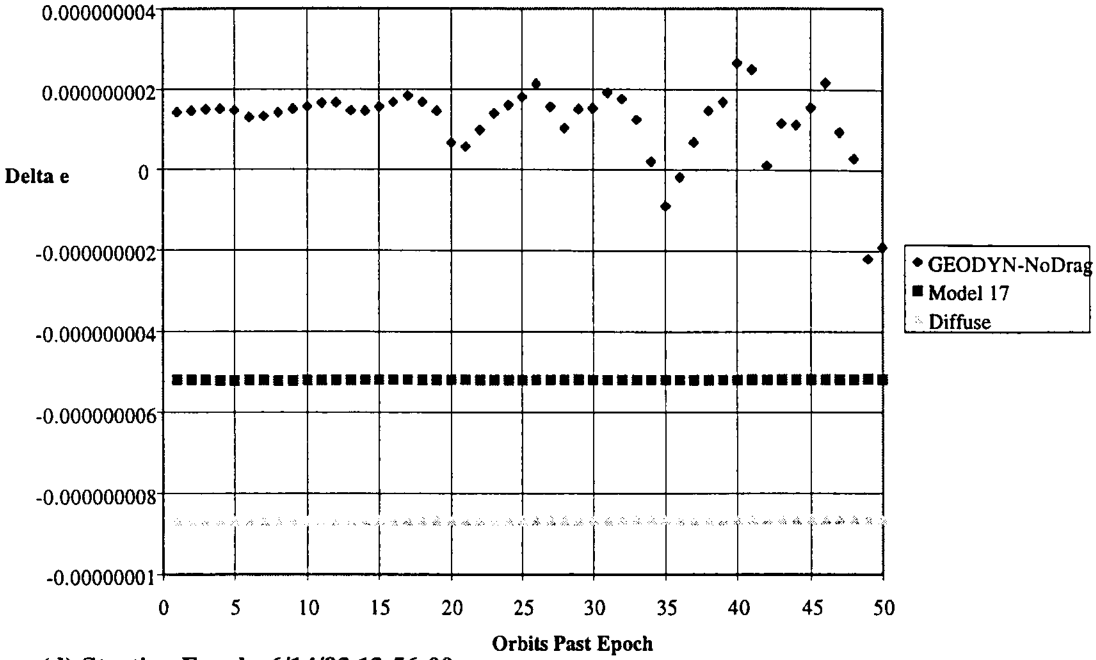

(d) Starting Epoch: 6/14/93 13:56:00

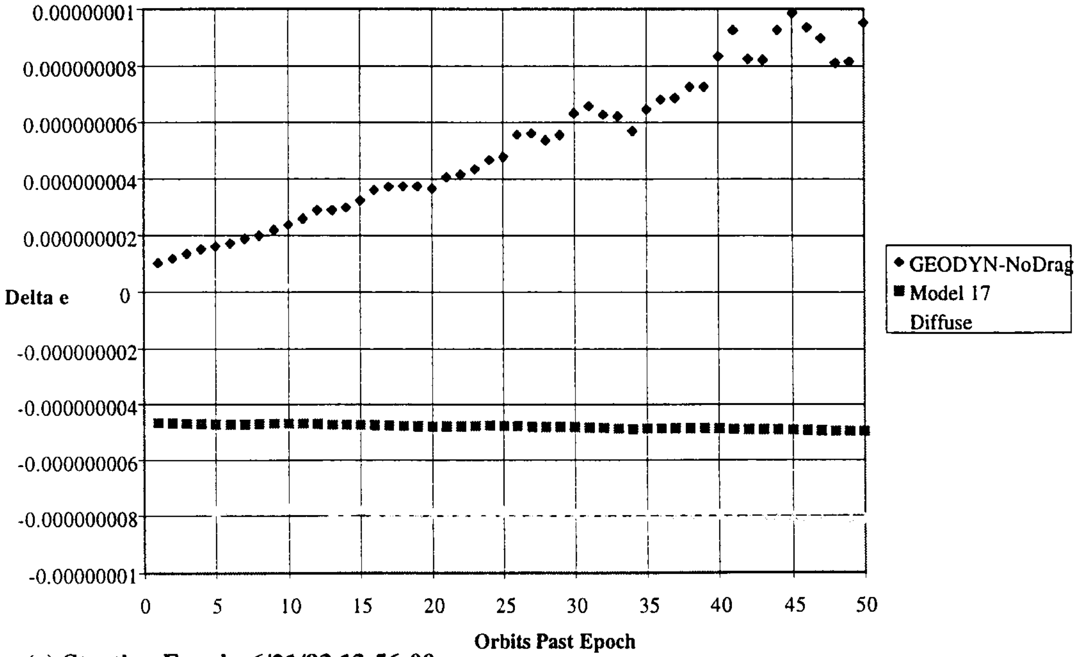

(e) Starting Epoch: 6/21/93 13:56:00

Figure 8. Change in Eccentricity (continued)

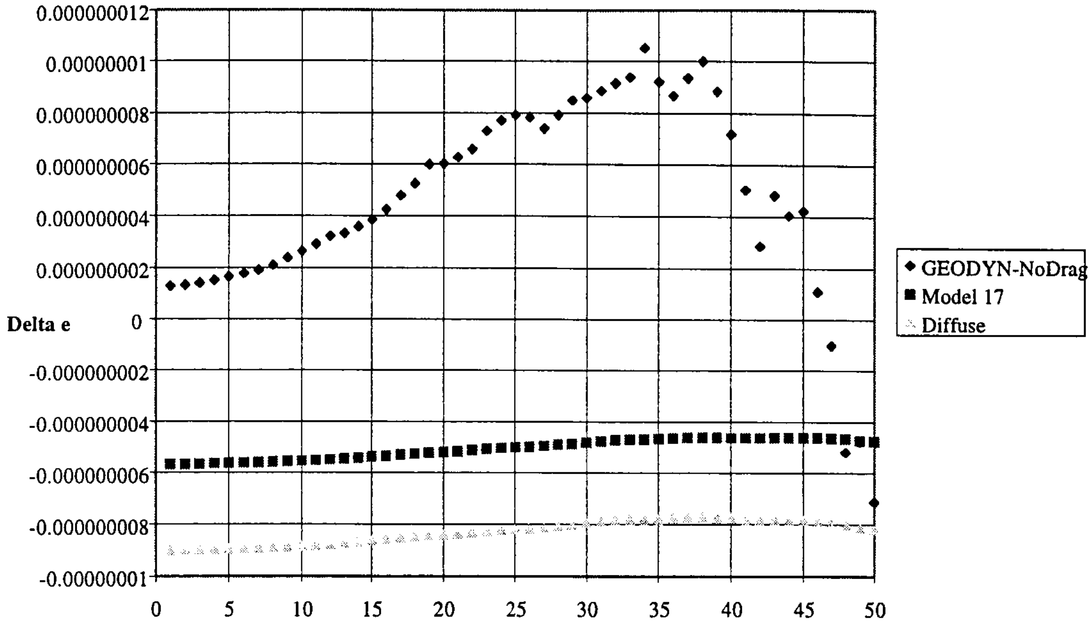

(f) Starting Epoch: 6/25/93 01:56:00

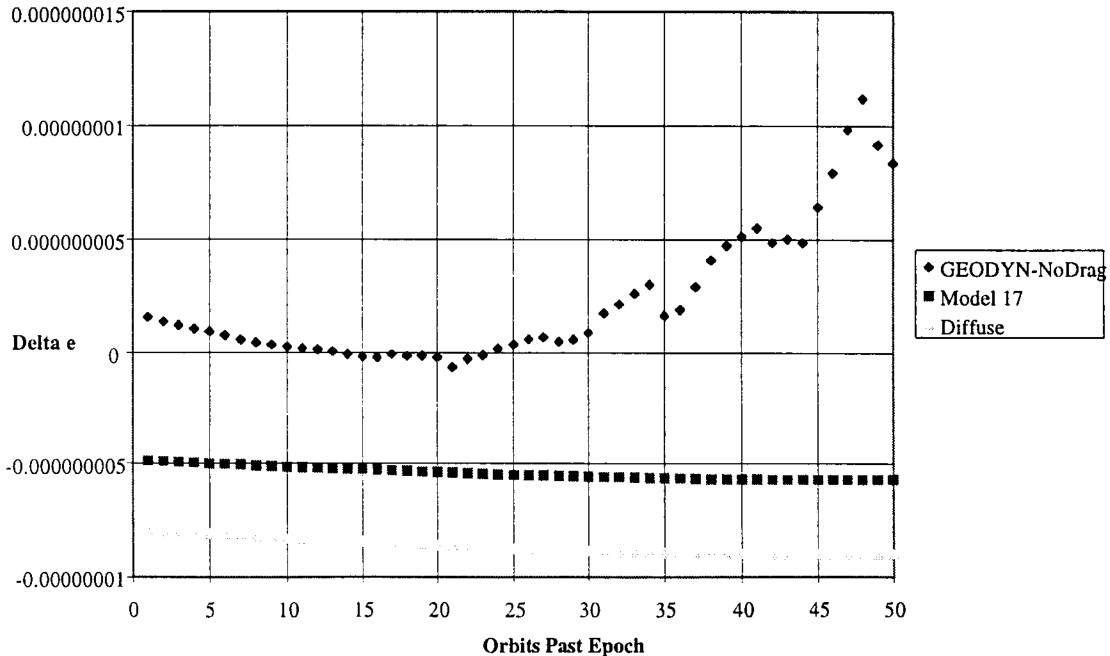

(g) Starting Epoch: 6/28/93 13:56:00

Figure 8. Change in Eccentricity (continued)

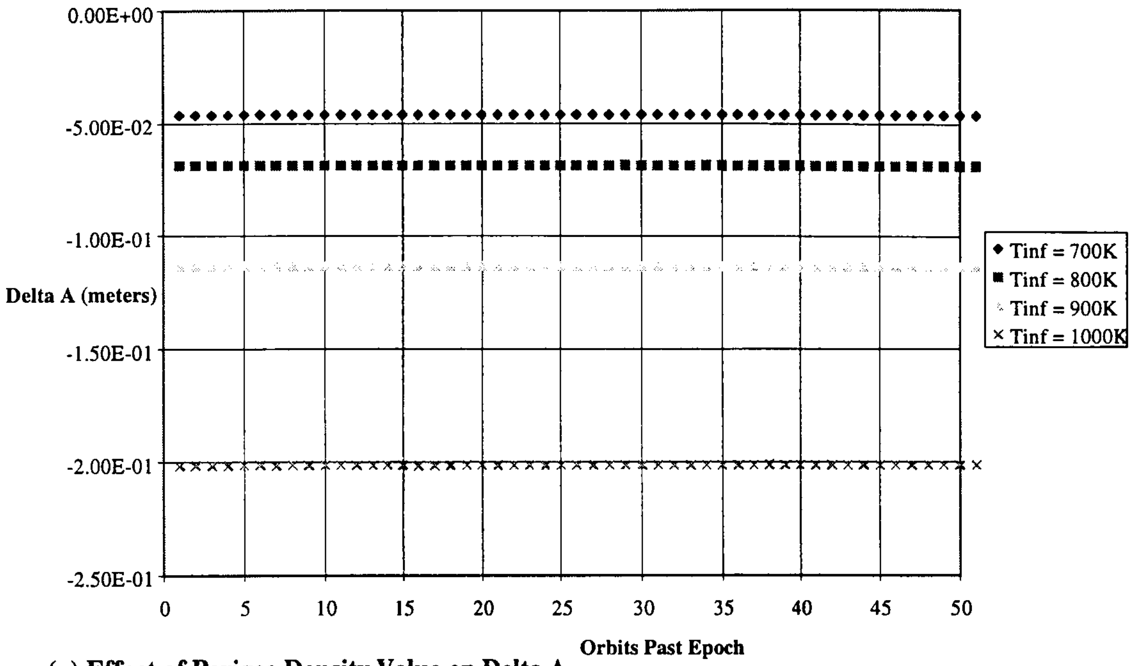

(a) Effect of Perigee Density Value on Delta A

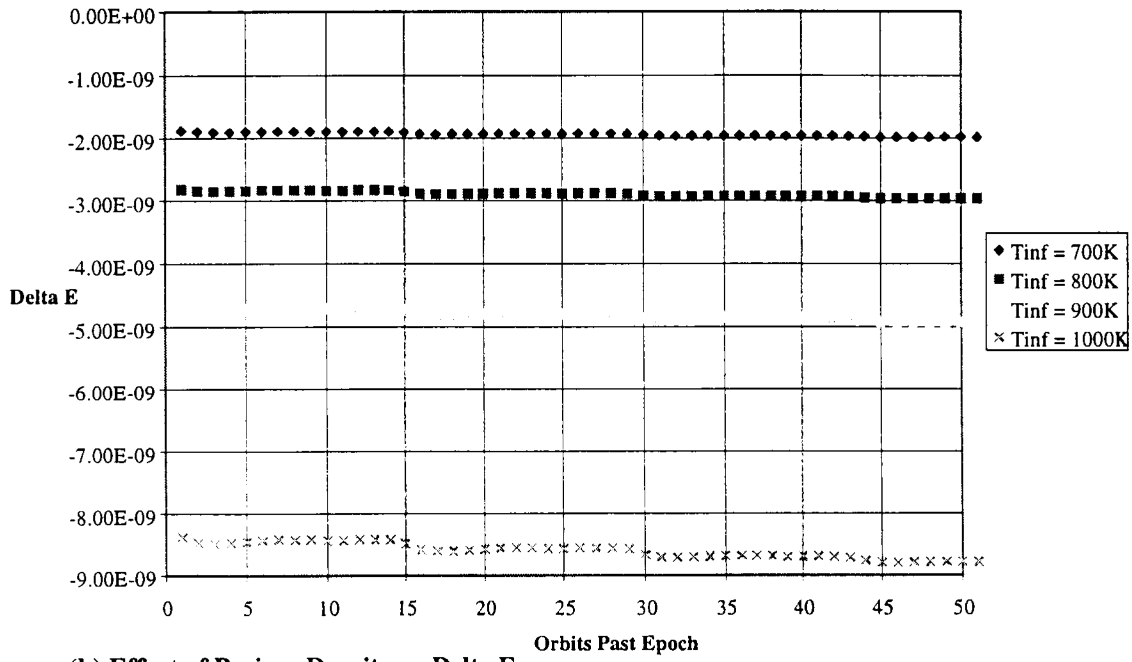

(b) Effect of Perigee Density on Delta E

Figure 9. Effect of Density on Perturbation Calculation

used in the Pert program obviously does not account for enough variation in the atmosphere to accurately predict the magnitude of the aerodynamic perturbations.

One approach to minimizing the effects of the atmospheric model on the prediction of aerodynamic perturbations has been demonstrated by Moore and Sowter (13). Their approach is to compare the ratio of two predicted perturbations. This should minimize the effect of the perigee density value on the predicted parameter, provided the variations in the atmosphere with respect to the density at that point are well modeled. The parameter $\Delta A/\Delta e$ is presented in Figure 10. Several of the cases shown show a good correlation between prediction models. Differences in density models are definitely minimized by examining the ratio of parameters, although some inaccuracy remains due to the fact that all the secular changes in the atmosphere are not modeled.

The last comparison that can be made is to look at whether the PERT aerodynamic model does a better job of recreating the Texas data than does the GEODYN aerodynamic model. Figure 11 shows the percent error in the prediction of the semi-major axis by the three prediction methods. The perturbed orbit used in the percent error calculation is calculated by summing the perturbations over an entire 3.5 day arc and adding this total perturbation to the NoDrag orbit. In many cases the predictions using the PERT calculations are slightly better than the GEODYN predictions. The percent error in eccentricity predictions is shown in Figure 12. Again the PERT predictions are slightly better in many cases. Figure 13 looks at the parameter $\Delta A/\Delta e$. Similar trends are shown by all three sets of data.

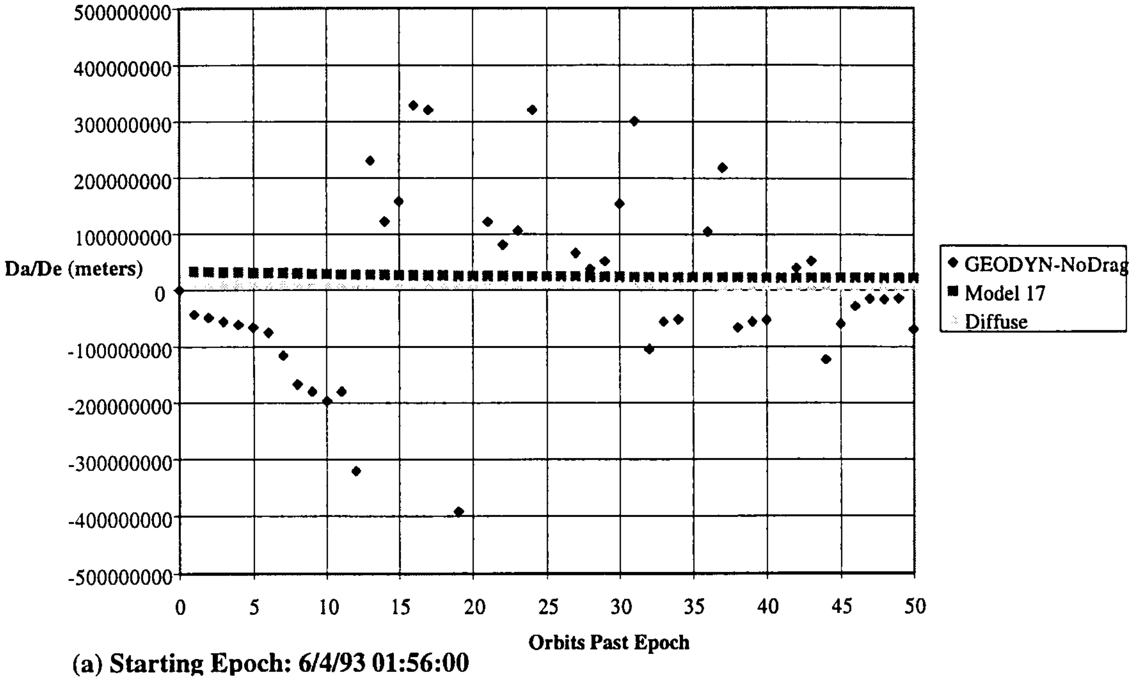

(a) Starting Epoch: 6/4/93 01:56:00

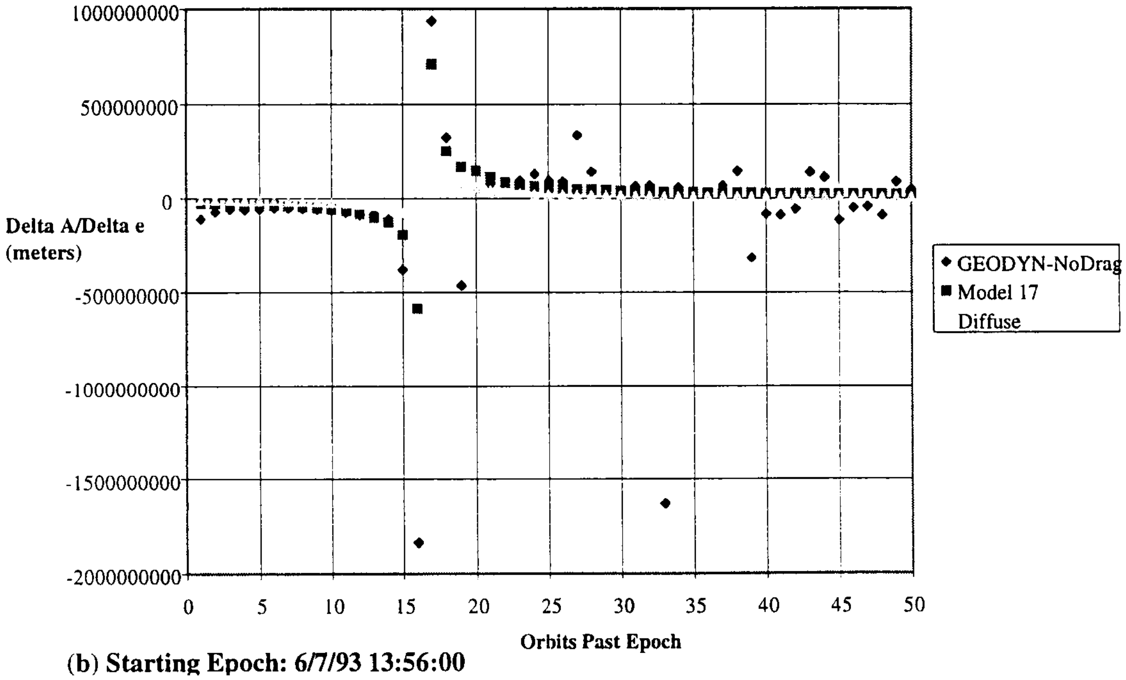

(b) Starting Epoch: 6/7/93 13:56:00

Figure 10. Delta A/ Delta e

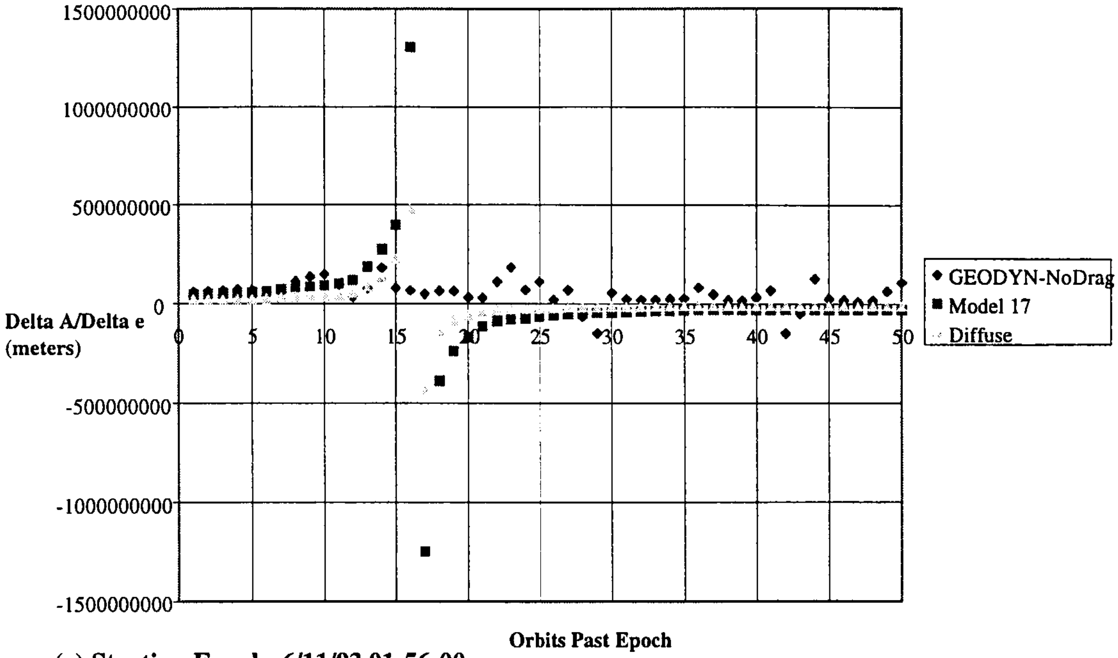

(c) Starting Epoch: 6/11/93 01:56:00

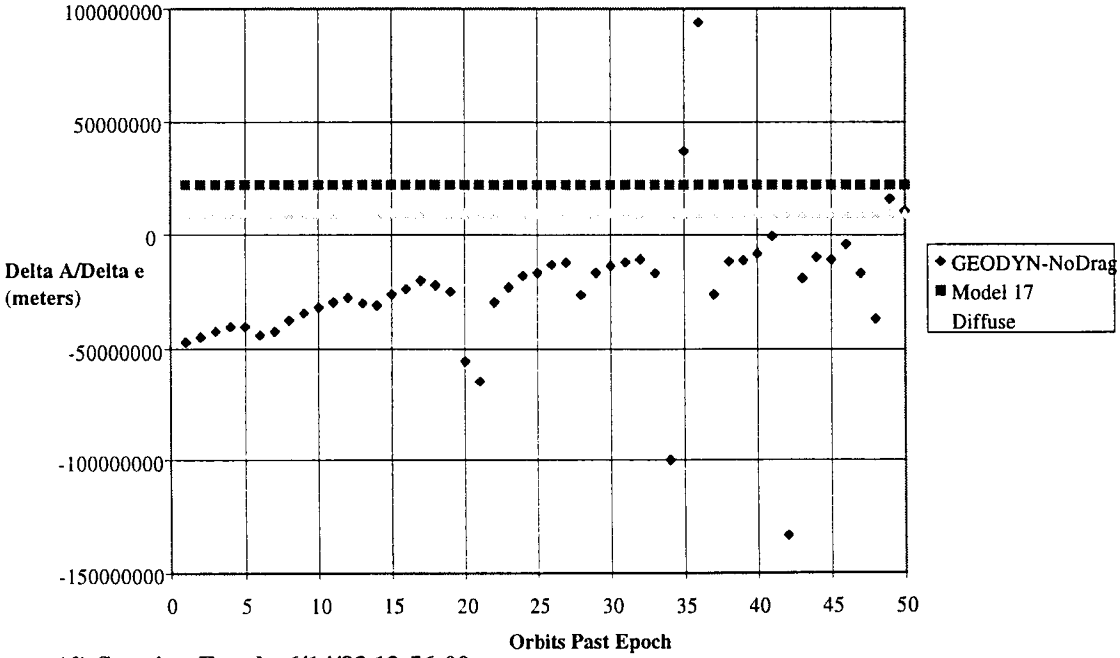

(d) Starting Epoch: 6/14/93 13:56:00

Figure 10. Delta A/ Delta e (continued)

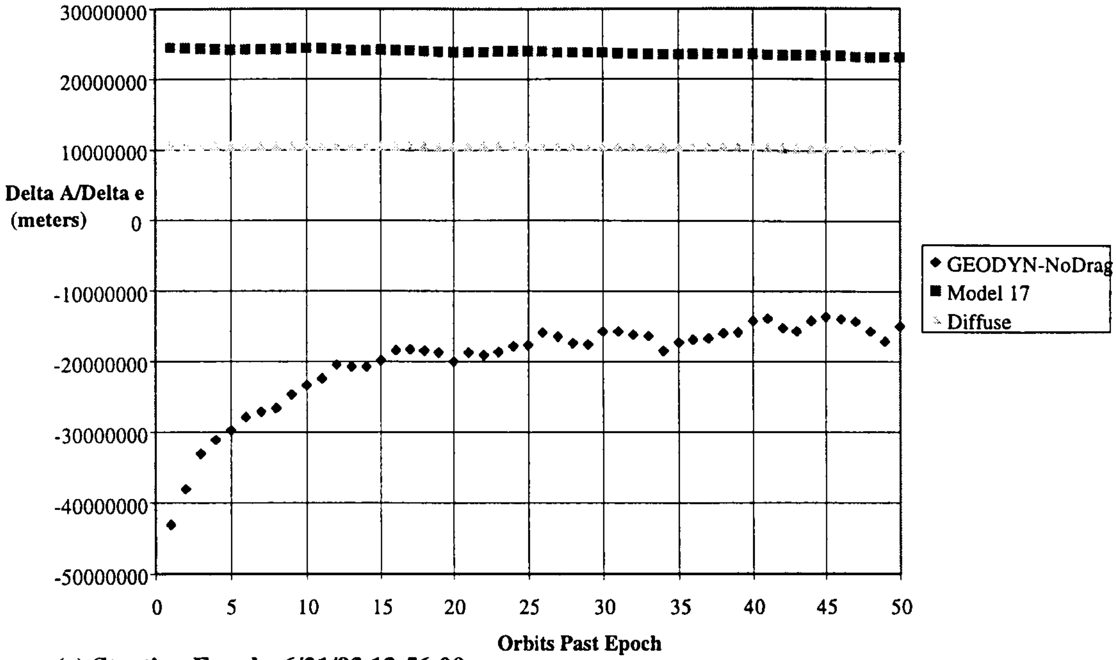

(e) Starting Epoch: 6/21/93 13:56:00

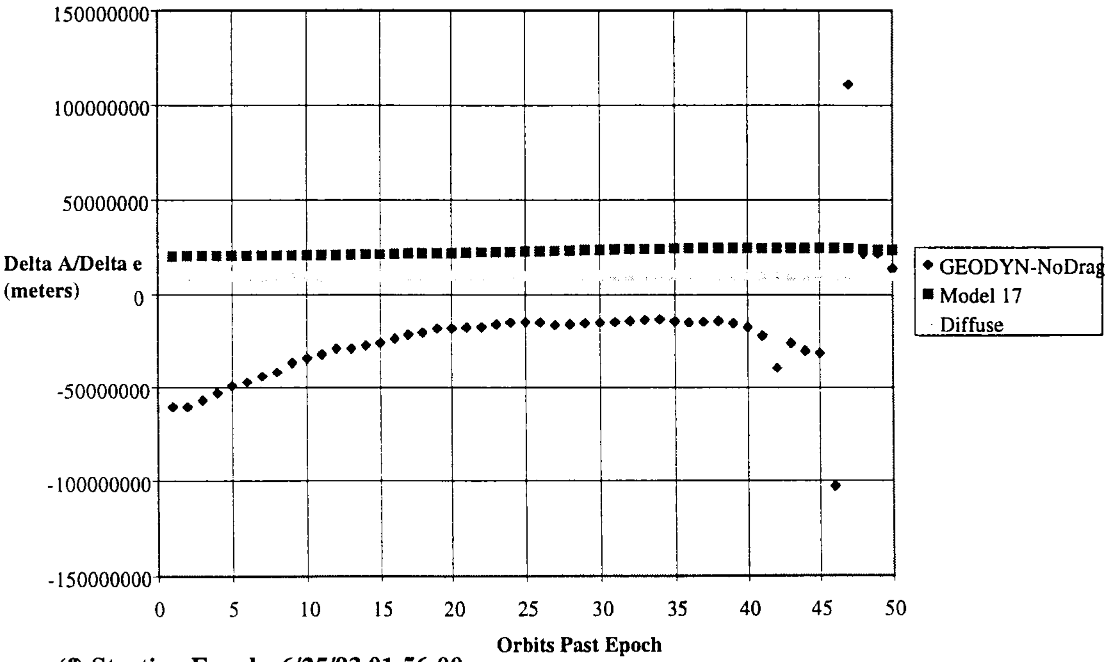

(f) Starting Epoch: 6/25/93 01:56:00

Figure 10. Delta A/ Delta e (continued)

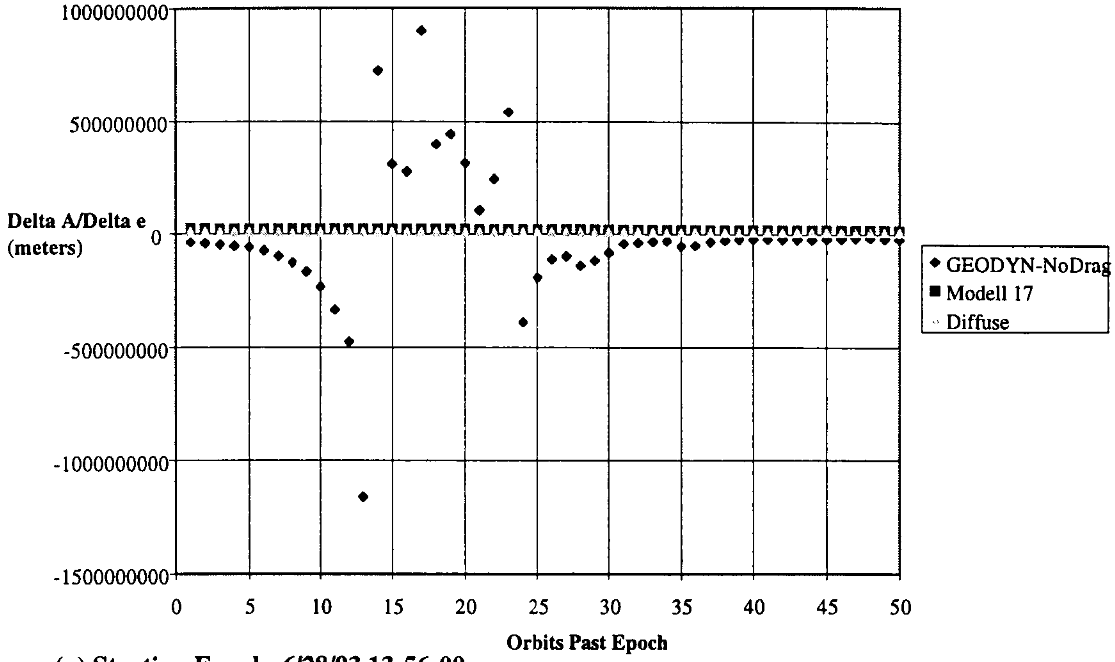

(g) Starting Epoch: 6/28/93 13:56:00

Figure 10. Delta A/ Delta e (continued)

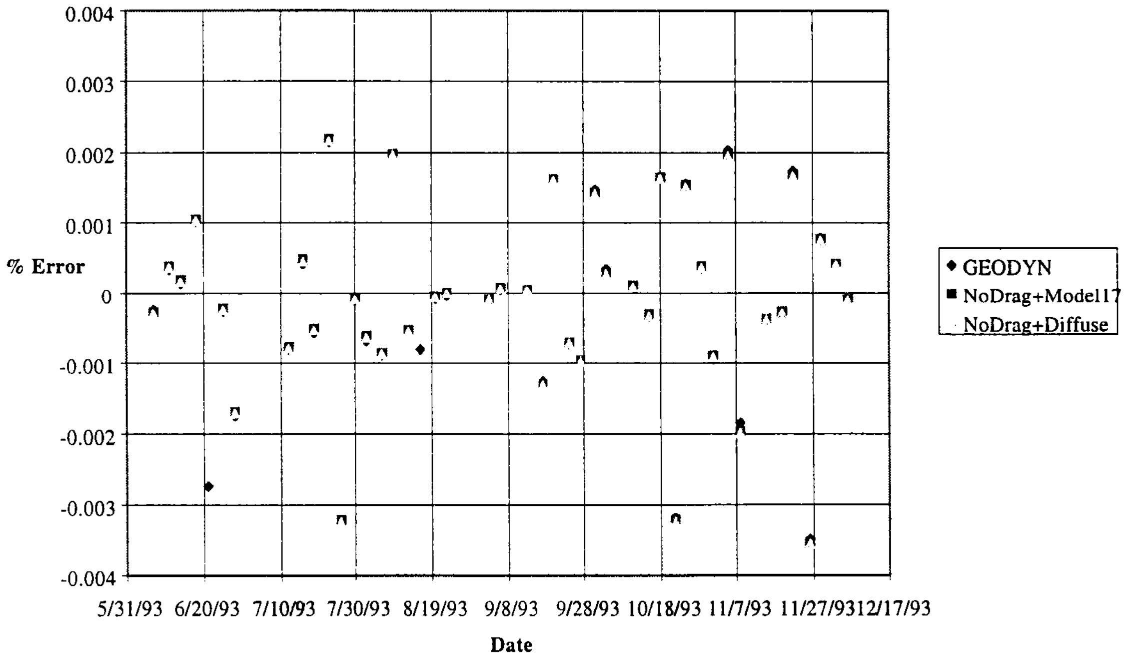

Figure 11. Comparision of Semi-Major Axis

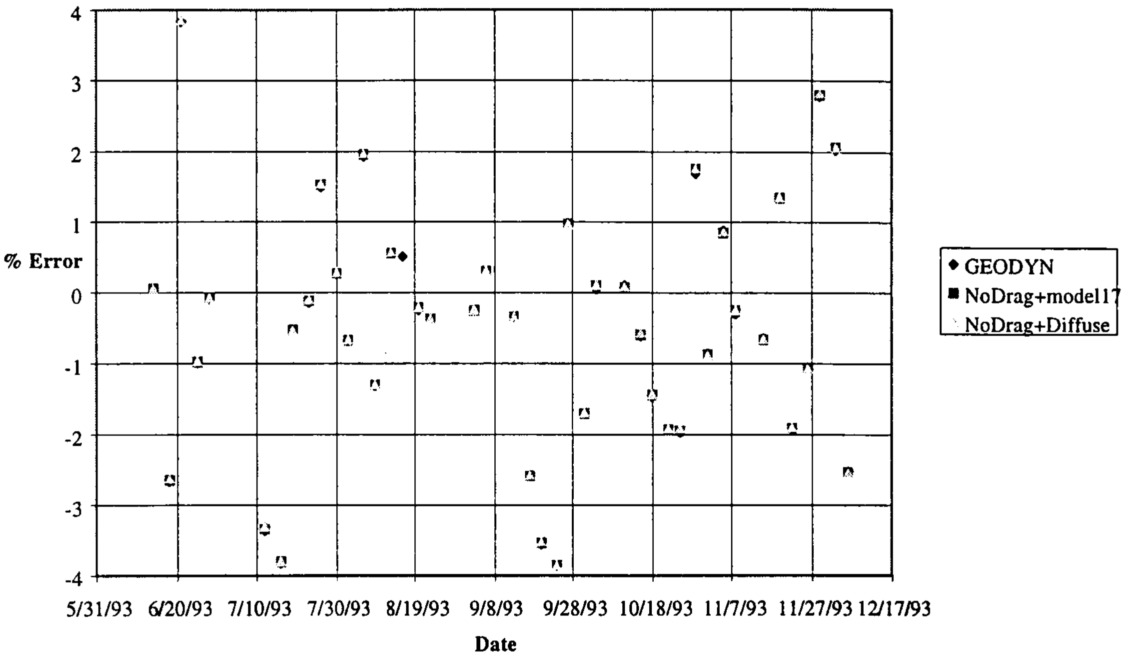

Figure 12. Comparision of Eccentricity

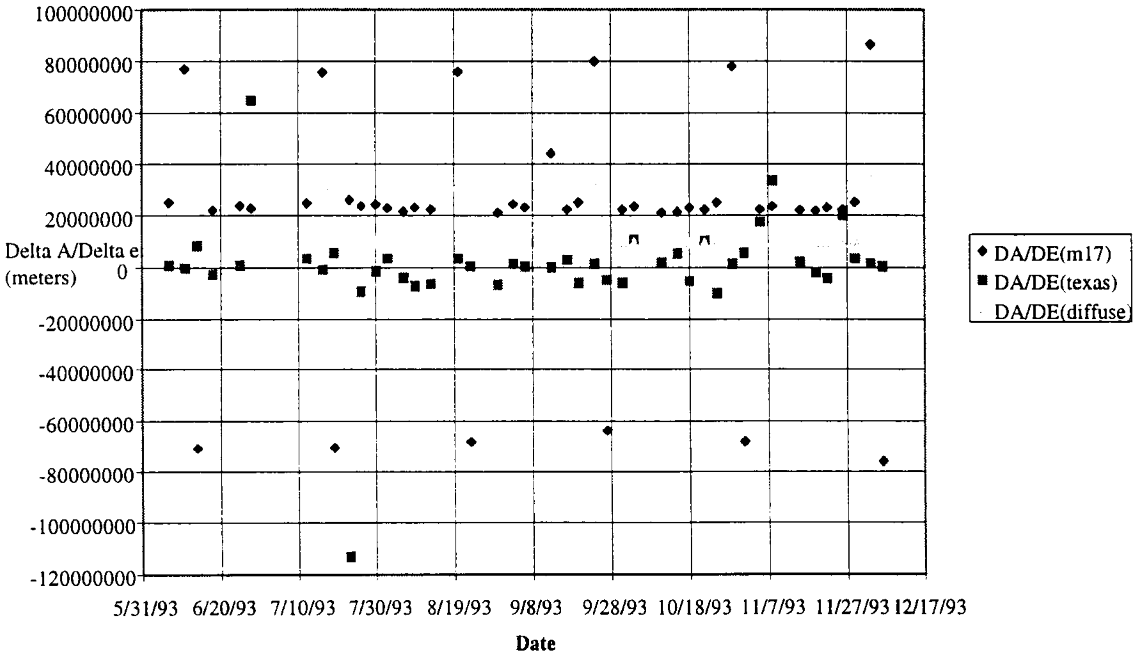

Figure 13. Comparision of Delta A/ Delta e

The points that are significantly away from the other points on Figure 13 warrant some discussion. These points correspond to cases where the calculated perturbation in eccentricity went from positive to negative resulting in much lower total perturbation for the 3.5 day arc. The variable model predictions are much greater in magnitude because of the contribution of the lift force in the eccentricity perturbation. We can see in Equation 3.8 that the lift and drag forces contribute in opposite directions to the eccentricity perturbation. It is inherent to the problem that a model that predicts a greater lift force will greatly effect the calculated perturbation. Comparison of corresponding points on Figures 12 and 13 show that the outlying points on Figure 13 correspond to points on Figure 12 where the percent error has been reduced.

Chapter V: Conclusions

It is quite apparent from this study that the gas-surface interaction can significantly effect the prediction of orbital perturbations. Current prediction methods that do not account for aerodynamic lift may inaccurately predict the change in the eccentricity of an orbit. The gas-surface interaction greatly influences the amount of lift produced by a body and needs to accounted for, especially if a satellite has large lift generating surfaces.

The most important factor when trying to predict the orbital perturbations on a satellite is the atmospheric model. A model such as the Jacchia 71 model that can account for the day to day variations in a baseline density value as well as variations due to latitude, time of day, and season should be used if at all possible. However, in many cases the ratio of two parameters can be used to minimize the effect of baseline density if a less accurate model is used.

Instruments being launched on many Earth observing satellites are requiring that orbits be predicted with centimeter and subcentimeter accuracy. Current prediction methods are only accurate within a few centimeters. Improvements in the prediction of the aerodynamic effects on the orbit could help to achieve this goal.

Two techniques are available to further improve and validate the aerodynamic model presented in this paper. The first involves incorporating the variable model for C_D and C_L into an orbit prediction program such as GEODYN. This routine could then be used when reducing tracking data and any improvement in the prediction of the orbit would immediately be obvious. To do this, a routine for calculating the force due to lift must be added to the program. Routines for predicting the lift and drag coefficients as a function of the satellite's position and orientation must also be included. These routines then must be called at the appropriate times by the main program integrating the orbit of the satellite.

The other approach uses telemetry data from the stabilizing flywheels used to maintain the satellite's orientation in orbit. This data can provide accurate measurements of the forces and torques experienced by the satellite. If this force data can be combined with accurate density measurements around the satellite an aerodynamic force model can be validated. If accurate density measurements are not available the approach of examining the ratio of parameters could be used.

References

References

(1) Schaaf, S. A., Chambre, P. L., Flow of Rarefied Gases, Princeton University Press, Princeton, 1961.

(2) Moe, K., "Absolute Atmospheric Densities Determined from the Spin and Orbital Decays of Explorer VI," Planetary and Space Sciences, Vol. 14, 1966, pp. 1065-1075.

(3) Crowther, R., and Stark, J., "The Determination of the Gas-Surface Interaction from Satellite Orbit Analysis as applied to ANS-1 (1975-70A)," Planetary and Space Sciences, Vol. 39, 1991, pp. 729-736.

(4) Collins, F. G., "Free Molecule Flow Gas/Surface Interactions at Orbital Conditions," Rarefied Gas Aerodynamic Bridging Procedures: SBIR Phase II Final Report, Vol. II, 1992, pp. 1-163.

(5) Knox, E. C., Collins, F. G., and Liver, P. A., "Engineering Assessment of Gas/Surface Interactions in Free-Molecule Aerodynamics," AIAA 91-1747.

(6) Bate, R. R., Mueller, D. D., White, J. E., Fundementals of Astrodynamics, Dover Publications, New York, 1971.

(7) Scharroo, R., Wakker, K. F., Ambrosius, A. C., Noomen, R., van Gaalen, W. J., Mets, G. J., "ERS-1 Precise Orbit Determination," AAS 93-270, pp. 293-307.

(8) Moore, P., Sowter, A., "Application of a Satellite Aerodynamics Model Based on Normal and Tangential Momentum Accommodation Coefficients," Planetary and Space Sciences, Vol. 39, 1991, pp. 1405-1419.

(9) Gentry, A. E., Smyth, D. N., and Oliver, W. R., "The Mark IV Supersonic-Hypersonic Arbitrary-Body Program," AFFDL-TR-73-159, Vol. 2, 1973.

(10) McCarthy, J. J., Rowton, S., Moore, D., Pavlis, D. E., Luthcke, S. B., Tsaoussi, L. S., "GEODYN II: Systems Description - Volume 1," NASA 1993.

(11) Francis, R., Graf, G., Edwards, P. G., McGain, M., McCarthy, C., Dubock, P., Lefebvre, A., Pieper, B., Pouvreau, P.-Y., Wall, R., Wechsler, F., Louet, J., and Zobl, R., "The ERS-1 Spacecraft and Its Payload," ESA Bulletin, No. 65, 1991, pp. 27-48.

(12) Holdaway, R., "Assessing Orbit Determination Requirements for ERS-1," AIAA 86-0403.

(13) Moore, P., Sowter, A., "Application of a Satellite Aerodynamics Model Based on Normal and Tangential Momentum Accommodation Coefficients," Planetary and Space Sciences, Vol. 39, 1991, pp. 1405-1419.

(14) Crowther, R., and Stark, J., "Determination of Momentum Accommodation from Satellite Orbits: An Alternative Set of Coefficients," AIAA 89-456

(15) Jacchia, L. G., "Revised Static Models of the Thermosphere and Exosphere with Empirical Temperature Profiles," SOA Special Report 332, May 1971.

(16) King-Hele, D., Satellite Orbits in an Atmosphere: Theory and Applications, Backie, London, 1983.

(17) U.S. Standard Atmosphere Supplements, 1966, U.S. Government Printing Office, Washington, DC, 1966.

Bibliography

Bibliography

The Astronomical Almanac for the Year 1993, U.S. Government Printing Office, Washington DC, 1992.

Bartel, T.J., Blackwell, B. F., and Sheldahl, R. E., "Measurement of the Freestream Density for Re-Entry Vehicles: A Design Study," 17th International Rarefied Gas Dynamics Symposium, 1990, pp. 1-7.

Bate, R. R., Mueller, D. D., White, J. E., Fundementals of Astrodynamics, Dover Publications, New York, 1971.

Blanchard, R. C., Phillips, W. P., Kelly, G. M., and Findlay, J. T., "Comparisons of Subsonic Drag Estimates Derived from Pioneer Venus Probes Flight Data with Wind-Tunnel Results," AIAA 80-1578.

Blanchard, R. C., and Walberg, G. D., "Determination of the Hypersonic-Continuum/Rarefied-Flow Drag Coefficient of the Viking Lander Capsule 1 Aeroshell from Flight Data," NASA Technical Paper 1793, 1980, pp.-57.

Blanchard, R. C., Duckett, R. J., and Hinson, E. W., "A Shuttle Upper Atmosphere Mass Spectrometer (SUMS) Experiment," AIAA 82-1334.

Blanchard, R. C., and Rutherford, J. F., "The Shuttle Orbiter High Resolution Accelerometer Package Experiment: Preliminary Flight Results," AIAA 84-0490.

Blanchard, R. C., and Buck, G. M., " Determination of Rarefied-Flow Aerodynamics of the Shuttle Orbiter from Flight Measurements on STS-6 and STS-7," AIAA 85-0347.

Blanchard, R. C., "Rarefied Flow Lift -To-Drag Measurements of the Shuttle Orbiter," A86-49123.

Blanchard, R. C., Hendrix, M. K., Fox, J. C., Thomas, D. O., and Nicholson, J., "The Orbital Acceleration Research Experiment," AIAA 86-1195.

Blanchard, R. C., and Larman, K. T., "Rarefied Aerodynamics and Upper Atmospheric Flight Results from the Orbiter High Resolution Accelerometer Package Experiment," AIAA 87-2366.

Blanchard, R.C., Hinson, E. W., and Nicholson, J. Y., "Shuttle High Resolution Accelerometer Package Experiment Results: Atmospheric Density Measurements Between 60-160 km," AIAA 88-0492.

Blanchard, R. C., and Hinson, E. W., "Rarefied-Flow Pitching Moment Coefficient Measurements of the Shuttle Orbiter," A89-13683.

Blanchard, R. C., Larman, K. T., and Moats, C. D., "Flight Calibration Assessment of HiRap Accelerometer Data," AIAA 93-0836.

Blanchard, R. C., Larman, K. T., and Moats, C. D., "Rarefied-Flow Shuttle Aerodynamics Flight Model," AIAA 93-3441.

Buck, G. M., and Blanchard, R. C., "Rarefied Aerodynamics and Upper Atmosphere Density from Multiple Orbiter Flight Measurements," AIAA 86-0269.

Champion, K. W., and Minzner, R. A., "Atmospheric Densities from Satellites and Rocket Observation," Planetary and Space Sciences, Vol. 1, 1959, pp. 259-264.

Chiang, K. C., Knuth, E. L., "Interactions of Hyperthermal Gas Particles with Contaminated Surfaces," The Journal of Chemical Physics, Vol. 53, 1970, pp. 2133-2142.

Chobotov, V. A. ed., Orbital Mechanics, American Institute of Aeronautics and Astronautics, Whashington, DC, 1991.

Collins, F. G., "Free Molecule Flow Gas/Surface Interactions at Orbital Conditions," Rarefied Gas Aerodynamic Bridging Procedures: SBIR Phase II Final Report, Vol. II, 1992, pp. 1-163.

Collins, F. G., Knox, E. C., "Parameters of Nocilla Gas/Surface Interaction Model from Measured Accommodation Coefficients," AIAA Journal, Vol. *, 1994, pp.

Collins, F. G., Knox, E. C., "Review of the Expected Magnitude of Aerodynamic Forces in Free-Molecule Flow," 1995.

Colquitt, E. S., Malyevac, C. W., and Anderle, R. J., "Doppler Computed Seasat Orbits," The Journal of the Astronautical Sciences, Vol. 28, 1980, pp. 391-403.

Compton, H. R., Blanchard, R. C., and Walberg, G. D., "An Experiment for Shuttle Aerodynamic Force Coefficient Determination from Inflight Dynamical and Atmospheric Measurements," AIAA 1978-795.

Compton, H. R., and Blanchard, R. C., "Shuttle Entry Trajectory Reconstruction Using Inflight Accelerometer and Gyro Measurements," AIAA 79-0257.

Crowther, R., and Stark, J., "Determination of Momentum Accommodation from Satellite Orbits: An Alternative Set of Coefficients," AIAA 89-456

Crowther, R., and Stark, J., "The Determination of the Gas-Surface Interaction from Satellite Orbit Analysis as applied to ANS-1 (1975-70A)," Planetary and Space Sciences, Vol. 39, 1991, pp. 729-736.

Eckels, A., Koidan, R., Harris, I., and Jastrow, R., "Ephemeris of Satellite 1957 Alpha 2," NASA Technical Memo 103090.

Faucher, G. A., and Procunier, R. W., "Upper-Atmosphere Density Obtained from Measurements of Drag on a Falling Sphere," Journal of Geophysical Research, Vol. 68, 1963, pp. 3437-3450.

Francis, R., Graf, G., Edwards, P. G., McGain, M., McCarthy, C., Dubock, P., Lefebvre, A., Pieper, B., Pouvreau, P.-Y., Wall, R., Wechsler, F., Louet, J., and Zobl, R., "The ERS-1 Spacecraft and Its Payload," ESA Bulletin, No. 65, 1991, pp. 27-48.

Fredo, R. M., and Kaplan, M. H., "Procedure for Obtaining Aerodynamic Properties of Spacecraft," Journal of Spacecraft and Rockets, Vol. 18, 1981, pp. 367-373.

Gentry, A. E., Smyth, D. N., and Oliver, W. R., "The Mark IV Supersonic-Hypersonic Arbitrary-Body Program," AFFDL-TR-73-159, Vol. 2, 1973.

Goad, C. C., Douglas, B. C., and Agreen, R. W., "On the Use of Satellite Altimeter Data for Radial Ephemeris Improvement," The Journal of the Astronautical Sciences, Vol. 28, 1980, pp. 419-428.

Hale, F. J., Introduction to Space Flight, Prentice Hall, Englewood Cliffs, 1994.

Harris, I., Jastrow, R., " An Interim Atmosphere Derived From Rocket and Satellite Data," Planetary and Space Sciences, Vol. 1, 1959, pp. 20-26.

Herrero, F. A., "The Lateral Surface Drag coefficient of Cylindrical Spacecraft in a Rarefied Finite Temperature Atmosphere," AIAA Journal, Vol. 23, 1985, pp. 862-867.

Holdaway, R., "Assessing Orbit Determination Requirements for ERS-1," AIAA 86-0403.

Imbro, D. R., Moe, M. M., and Moe, K., "On Fundamental Problems in the Deduction of Atmospheric Densities from Satellite Drag," Journal of Geophysical Research, Vol. 80, 1975, pp. 3077-3086.

Jacchia, L. G., "Revised Static Models of the Thermosphere and Exosphere with Empirical Temperature Profiles," SOA Special Report 332, May 1971.

Jacchia, L. G., "Thermospheric Temperature, Density, and Composition: New Models," SOA Special Report 375, March 1977.

Karr, G. R., Cleland, J. G., and DeVries, L. L., "Aerodynamic Lift Effect on Satellite Orbits," AIAA 75-12.

King-Hele, D., Satellite Orbits in an Atmosphere: Theory and Applications, Backie, London, 1983.

Klinkrad, H., "A Semi-Analytical Theory for Precise Single Orbit Predictions of ERS-1," Space Dynamics; Proceedings of the International Symposium, 1989, pp. 575-600.

Knox, E. C., and Jain, A. C., "Technical Summary for Improved Rarefied Gas Aerodynamic Bridging Procedures," Rarefied Gas Aerodynamic Bridging Procedures: SBIR Phase II Final Report, Vol. 1, 1992, pp. 1-89.

Knox, E. C., Collins, F. G., and Liver, P. A., "Engineering Assessment of Gas/Surface Interactions in Free-Molecule Aerodynamics," AIAA 91-1747.

Marsh, J. G., and Williamson, R. G., "Precision Orbit Analyses in Support of the Seasat Altimeter Experiment," The Journal of the Astronautical Sciences, Vol. 28, 1980, pp. 345-369.

McCarthy, D. D., "IERS Standards (1992)," IERS Technical Note 13, July 1992.

McCarthy, J. J., Rowton, S., Moore, D., Pavlis, D. E., Luthcke, S. B., Tsaoussi, L. S., "GEODYN II: Systems Description - Volume 1," NASA 1993.

Moe, K., "Absolute Atmospheric Densities Determined from the Spin and Orbital Decays of Explorer VI," Planetary and Space Sciences, Vol. 14, 1966, pp. 1065-1075.

Moe, K., "Recent Experimental Evidence Bearing on Satellite Drag Coefficients," AIAA Journal, Vol. 6, 1968, pp. 1375-1377.

Moe, M. M., and Moe, K., "The Roles of Kinetic Theory and Gas-Surface Interactions in Measurements of Upper-Atmospheric Density," Planetary and Space Sciences, Vol. 17, 1969, pp. 7-922.

Mohan, S. N., Bierman, G. J., Hamata, N. E., and Stavert, R. L., "Seasat Orbit Refinement for Altimetry Application," The Journal of the Astronautical Sciences, Vol. 28, 1980, pp. 405-417.

Moore, P., "The Effect of Aerodynamic Lift on Near-Circular Satellite Orbits," Planetary and Space Sciences, Vol. 33, 1985, pp. 479-491.

Moore, P., Sowter, A., "Application of a Satellite Aerodynamics Model Based on Normal and Tangential Momentum Accommodation Coefficients," Planetary and Space Sciences, Vol. 39, 1991, pp. 1405-1419.

Moore, P., Sowter, A., "Variations in the Normal and Tangential Momentum Accommodation Coefficients from Analysis of Atmospheric Lift and Drag Forces on ANS-1 (1974-70A)," Advances in Space Research, Vol. 10, 1990, pp. 311-316.

Nerem, R. S., Marshall, J. A., Putney, B. H., Pavlis, E. C., Klosko, S. M., Williamson, R. G., and Zelensky, N. P., "Precision Orbit Determination for the Topex/Poseidon Mission," AIAA, 1992.

Oza, D. H., Jones, T. L., Hakimi, M., Samii, M. V., Doll, C. E., Mistretta, G. D., and Hart, R. C., "LANDSAT-4 (TDRSS-USER) Orbit Determination using Batch Least-Squares and Sequential Methods," AIAA 92-4432.

Price, J. M., Blanchard, R. C., " Determination of Atmospheric Properties for STS-1 Aerothermodynamic Investigations," AIAA 81-2430.

Putney, B., Kolenkiewicz, R., Smith, D., Dunn, P., and Torrence, M. H., "Precision Orbit Determination at the NASA Goddard Space Flight Center," Advances in Space Research, Vol. 10, 1990, pp. 197-203.

Rault, D. F. G., "Aerodynamics of Shuttle Orbiter at High Altitudes," AIAA, 1993.

Reiter, G. S., Moe, K., "Surface-Particle -Interaction Measurements Using Paddlewheel Satellites," Sixth Rarefied Gas Dynamics, 1969, pp. 1543-1555.

Rogers, M. J. B., Baugher, C. R., Blanchard, R. C., DeLombard, R., Durgin, W. W., Matthiesen, D. H., Neupert, W., and Roussel, P., "Low Gravity Environment On-board Columbia During STS-40," AIAA 93-0833.

Schaaf, S. A., Chambre, P. L., Flow of Rarefied Gases, Princeton University Press, Princeton, 1961.

Scharroo, R., Wakker, K. F., Ambrosius, A. C., Noomen, R., van Gaalen, W. J., Mets, G. J., "ERS-1 Precise Orbit Determination," AAS 93-270, pp. 293-307.

Schilling, G. F., Whitney, C. A., "Derivation and Analysis of Atmospheric Density from Observations of Satellite 1958m Epsilon," Planetary and Space Sciences, Vol. 1, 1959, pp. 136-145.

Schutz, B. E., Tapley, B. D., Eanes, R. J., Marsh, J. G., Williamson, R. G., and Martin, T. V., "Precision Orbit Determination Software Validation Experiment," The Journal of the Astronautical Sciences, Vol. 28, 1980, pp. 327-343.

Schutz, B. E., and Tapley, B. D., "Orbit Accuracy Assessment of Seasat," The Journal of the Astronautical Sciences, Vol. 28, 1980, pp. 371-390.

Schutz, B. E., "Precise Seasat Ephemeris from Laser and Altimeter Data," Advances in Space Research, Vol. 5, 1984, pp. 155-168.

Siry, J. W., "Satellite Orbits and Atmospheric Densities at Altitudes up to 750 km Obtained from the Vanguard Orbit Determination Program," Planetary and Space Sciences, Vol. 1, 1959, pp. 184-192.

Stirton, R. J., "The Upper Atmosphere and Satellite Drag," Smithsonian Contributions to Astrophysics, Vol. 5, 1960, pp. 9-15.

Stark, J., "Aerodynamic Modeling of Spacecraft for Precise Orbit Determination," Proceedings of the Second International Symposium on Spaceflight Dynamics, 1986, pp. 20-23.

Tapley, B. D., and Born, G. H., "The Seasat Precision Orbit Determination Experiment," The Journal of the Astronautical Sciences, Vol. 28, 1980, pp. 315-326.

Thompson, J. M., Russell, J. W., and Blanchard, R. C., "Methods for Extracting Aerodynamic Accelerations from Orbiter High Resolution Accelerometer Package Flight Data," AIAA 87-2365.

U.S. Standard Atmosphere Supplements, 1966, U.S. Government Printing Office, Washington, DC, 1966.

Vigue, Y., Lichten, S. M., Muellerschoen, R. J., Blewitt, G., and Heflin, M. B., "Improved GPS Solar Radiation Pressure Modeling for Precise Orbit Determination," Journal of Spacecraft and Rockets, Vol. 31, 1994, pp. 830-833.

Wakker, K. F., "Orbit Prediction for the Astronomical Netherlands Satellite," Journal of the British Interplanetary Society, Vol. 31, 1978, pp. 387-397.

Warwick, J. W., "Decay of Sputnik I," Planetary and Space Sciences, Vol. 1, 1959, pp. 43-49.

Wiesel, W. E., Spaceflight Dynamics, McGraw-Hill Inc, New York, 1989

Wu, Jain-Ming, "On a Near-Earth Satellite Theory," Proceedings of the Tenth International Symposium on Space Technology and Science, 1973, pp.349-364.

Zmievskaya, G. I., and Pyampuu, A. A., "Determination of the Aerodynamic Characteristics of a Satellite with Consideration of the Mechanism of Surface Interaction," Kosmicheskie Issledovaniya, Vol. 12, 1974, pp. 55-61.

Appendices

Appendix A: Computer Programs

A.1 THETA.F

```
C       DEFINE VARIABLES

        REAL THETA, OMEGA, T, TO, TG
        REAL THR, TMIN, TSEC
        REAL TOHR, TOMIN, TOSEC
        REAL TGHR, TGMIN, TGSEC,DELTAA
        REAL YEAR, MONTH, DAY
        CHARACTER*6 LABEL
        REAL X, Y, Z, XDOT, YDOT, ZDOT
        REAL TEMPX, TEMPY, TEMPZ
        INTEGER NOBS, I

C       READ DATA CARD

        OPEN(9, FILE="texas.eph2")
        NOBS=58
        DO 500 I=1,NOBS

        READ(9,10) LABEL, YEAR, MONTH, DAY
        READ(9,10) LABEL, THR, TMIN, TSEC
        READ(9,10) LABEL, X, Y, Z
        READ(9,10) LABEL, XDOT, YDOT, ZDOT

 10     FORMAT (10X,A6,4X,3E20.13)

C       PRINT EPOCH OF OBSERVATION

        WRITE(6,20) YEAR, MONTH, DAY
 20     FORMAT('DATE OF OBSERVATION ',3F10)

C       READ THETAG FROM KEYBOARD

        WRITE(6,30)
 30     FORMAT('ENTER HOUR FOR THETAG :')
        READ(5,40) TGHR
 40     FORMAT(F2)
        WRITE(6,50)
 50     FORMAT('ENTER MINUTE FOR THETAG: ')
        READ(5,40) TGMIN
        WRITE(6,60)
 60     FORMAT('ENTER SECONDS FOR THETAG: ')
        READ(5,70) TGSEC
 70     FORMAT(F7)
        WRITE(6,80) TGHR, TGMIN, TGSEC
 80     FORMAT('THETAG: ', 2F3,F7.4)
```

```
C        WRITE(6,90)
C 90     FORMAT('ENTER DELTA A (SEC):')
C        READ(5,40) DELTAA

C       CONVERT T, T0, AND TG TO SECONDS

        T=TSEC+(60*TMIN)+(60*60*THR)
C        T0=T0SEC+(60*TOMIN)+(60*60*TOHR)
        TG=TGSEC+(60*TGMIN)+(60*60*TGHR)

C       CALCULATE THETA

        OMEGA = 7.2921151467E-05
        THETA= OMEGA*(T+TG)

C       CONVERT POSITION VECTOR

        TEMPX=X*COS(THETA)-Y*SIN(THETA)
        TEMPY=X*SIN(THETA)+Y*COS(THETA)
        TEMPZ=Z
        X=TEMPX
        Y=TEMPY
        Z=TEMPZ

C       CONVERT VELOCITY VECTOR

        TEMPX=(XDOT*COS(THETA)-YDOT*SIN(THETA))
        TEMPY=(XDOT*SIN(THETA)+YDOT*COS(THETA))
        TEMPZ=ZDOT
        XDOT=TEMPX
        YDOT=TEMPY
        ZDOT=TEMPZ

C       PRINT POSITION AND VELOCITY IN GEODYN FORM

        WRITE(10,130) X,Y,Z
  130   FORMAT('ELEMS114',2X,'0300',6X,3D20.14)
        WRITE(10,140) XDOT,YDOT,ZDOT
  140   FORMAT('ELEMS2',14X,3D20.14)

  500   CONTINUE

        END
```

A.2 PERT.F

```
C      ******************************
C      * PERT- ORBITAL PERTURBATION *
C      *      PROGRAM               *
C      ******************************

       REAL*8 A,E,I, BIGOMEGA,OMEGA,MEAN
       REAL*8 ANGLE, DELTAA, DELTAE, DELTAAN, DELTAEN, H,
DYDX0
       CHARACTER DATE*22, HEADER*10
       COMMON A,E,I,MEAN,OMEGA
       INTEGER N, NMAX, M

       NMAX=1000

C      **** READ HEADERS FROM DATA FILE ***
       OPEN(5, FILE="fort.05")
       READ(5,10) HEADER
       READ(5,10) HEADER
 10    FORMAT(A10)
       WRITE(10,15)
 15    FORMAT('DATE',T28,'DELTAA',T57,'DELTAE')

       DO 50 M=1,51

C      *** READ ORBITAL ELEMENTS ****
          READ(5,20) DATE,A,E,I,BIGOMEGA,OMEGA, MEAN
 20
FORMAT(A22,5X,F11.3,2X,F13.11,4X,F12.9,4X,F13.9,4X,F13.9,4X,
F14.9)

          OMEGA=OMEGA*(3.14159265359/180.0)
          MEAN=MEAN*(3.14159265359/180.0)
          I=I*(3.14159265359/180.0)

          DELTAA=0.0
          DELTAE=0.0
          ANGLE=MEAN
          H=6.28318530718/NMAX
          DO 30 N=1,NMAX+1
             CALL DADE(ANGLE,DELTAA, DYDX0)
             CALL RK4(DELTAA,DYDX0,ANGLE,H,DELTAAN,DADE)
             CALL DEDE(ANGLE,DELTAE,DYDX0)
             CALL RK4(DELTAE,DYDX0,ANGLE,H,DELTAEN,DEDE)
             DELTAA=DELTAAN
             DELTAE=DELTAEN
             ANGLE=ANGLE+H
```

```
            IF(N .EQ. NMAX+1) THEN
               WRITE(10,25) DATE,DELTAA,DELTAE
 25            FORMAT(A22,E20.10,2X,E20.10)

            ENDIF

 30       CONTINUE

 50    CONTINUE

       STOP
       END

       SUBROUTINE DRAG(ANGLE,CD)

       COMMON A,E,I,MEAN,OMEGA
       REAL*8 CD,THETA

       THETA=ANGLE+OMEGA
       IF (THETA .GT. 6.28318530718) THETA=THETA-
6.28318530718

C      *** MODEL 17 CURVEFIT  ***
       CD= 1.11743+1.26263*SIN(THETA)+2.65699*SIN(THETA)**2

       RETURN
       END

       SUBROUTINE LIFT(ANGLE, CL)

       REAL*8 ANGLE, CL, THETA, THETAX
       COMMON A,E,I,MEAN,OMEGA

       THETA=ANGLE+OMEGA
       IF (THETA .GT. 6.28318530718) THETA=THETA-
6.28318530718

       IF (THETA .GT. 0.0) THEN
          THETAX=THETA/2.0

CL=0.658977*SIN(THETAX)+0.0114795*(THETAX*360/3.14159265359)
*
     1    SIN(THETAX)-
0.00406447*(THETAX*360/3.14159265359)*SIN(THETAX)**2
       ENDIF

       IF (THETA .GT. 1.5707963268) THEN
          THETAX=(3.14159265359-THETA)/2.0
          CL=-
(0.658977*SIN(THETAX)+0.0114795*(THETAX*360/3.14159265359)*
     1    SIN(THETAX)-
0.00406447*(THETAX*360/3.14159265359)*SIN(THETAX)**2)
```

```
      ENDIF

      IF (THETA .GT. 3.14159265359) THEN
         THETAX=(THETA-3.14159265359)/2.0
         CL=-
(0.658977*SIN(THETAX)+0.0114795*(THETAX*360/3.14159265359)*
     1     SIN(THETAX)-
0.00406447*(THETAX*360/3.14159265359)*SIN(THETAX)**2)
      ENDIF

      IF (THETA .GT. 4.71238898038) THEN
         THETAX=(6.28318530718 - THETA)/2.0

CL=0.658977*SIN(THETAX)+0.0114795*(THETAX*360/3.14159265359)
*
     1     SIN(THETAX)-
0.00406447*(THETAX*360/3.14159265359)*SIN(THETAX)**2
      ENDIF

      RETURN
      END

      SUBROUTINE DENSITY(ANGLE, RHO)

      REAL*8 RHO0, ANGLE, RHO,I,A,E,OMEGA
      REAL*8 K1,C,Z,RP,KAPPA,SCALEH
      COMMON A,E,I,MEAN,OMEGA

C     *** Tinf 900K ***
      RHO0=7.628E-15
      KAPPA=0.00335
      SCALEH=191590.0

C     *** KING-HELE OBLATE ATMOSPHERIC MODEL ***
      Z=A*E/SCALEH
      RP=(1.0-E)*A
      C=0.5*(RP*KAPPA/SCALEH)*SIN(I)**2
      K1=EXP(-Z*C*COS(2.0*OMEGA))


RHO=RHO0*K1*EXP(Z*COS(ANGLE))*(1.0+C*COS(2.0*(OMEGA+ANGLE))-
2.0*C*E*
     1
SIN(2.0*(OMEGA+ANGLE))*SIN(ANGLE)+0.25*C*C*(1.0+COS(4.0*(OME
GA+ANGLE))))

      RETURN
      END

      SUBROUTINE DADE(ANGLE, DUMMY, DELTAA)

      COMMON A,E,I,MEAN,OMEGA
      REAL*8 MU, ANGLE, DELTAA, S, A, E
```

```
      REAL*8 RHO, CD, MASS,V2, V, R, FD

      CALL DENSITY(ANGLE, RHO)
      CALL DRAG(ANGLE, CD)
      S=36.0
      MU=3.986004359E14
      MASS=1900.0

      V2=(MU/(A*(1.0-E*E)))*(1.0+E*COS(ANGLE))/(1.0-
E*COS(ANGLE))
      V=SQRT(V2)
      R=A*(1.0-E*COS(ANGLE))
      FD=-0.5*RHO*CD*S*V2/MASS

      DELTAA=(2.0*R*A*A*V/MU)*SQRT(A/MU)*FD

      RETURN
      END

      SUBROUTINE DEDE(ANGLE, DUMMY, DELTAE)

      COMMON A,E,I,MEAN,OMEGA
      REAL*8 MU, ANGLE,DUMMY,DELTAE,S,A,E,MASS
      REAL*8 RHO,CD,CL,V2,V,R,FD,FL

      CALL DRAG(ANGLE,CD)
      CALL LIFT(ANGLE,CL)
      CALL DENSITY(ANGLE, RHO)
      S=36.0
      MU=3.986004359E14
      MASS=1900.0

      V2=(MU/(A*(1.0-E*E)))*(1.0+E*COS(ANGLE))/(1.0-
E*COS(ANGLE))
      V=SQRT(V2)
      R=A*(1.0-E*COS(ANGLE))
      FD=-0.5*RHO*CD*S*V2/MASS
      FL=0.5*RHO*CL*S*V2/MASS

      DELTAE=(R/V)*SQRT(A/MU)*(2.0*FD*(E+(A/R)*(COS(ANGLE)-
E))+FL*SQRT(1.0-E*E)
     1    *SIN(ANGLE))

      RETURN
      END

      SUBROUTINE RK4(Y,DYDX,X,H,YOUT,DERIVS)

      REAL*8 Y,DYDX,X,YOUT,YT,DYT,DYM
      REAL*8 H, HH,H6,XH

      HH=H*0.5
      H6=H/6
```

```
XH=X+HH

YT=Y+HH*DYDX
CALL DERIVS(XH,YT,DYT)
YT=Y+HH*DYT
CALL DERIVS(XH,YT,DYM)
YT=Y+H*DYM
DYM=DYT+DYM
CALL DERIVS(X+H,YT,DYT)
YOUT=Y+H6*(DYDX+DYT+2*DYM)

RETURN
END
```

Appendix B: Comparision of Forces

One of the problems with trying to determine the forces acting to perturb a satellite's orbit is that many of these forces are of the same magnitude. It is often difficult to determine what forces are actually causing a perturbation. Assumptions made in one modeling one perturbation can mask errors in the modeling of other perturbations.

The data available on satellite orbits also makes it difficult to determine perturbing forces. Aerodynamic and solar radiation forces change perturb an orbit only a few centimeters over one revolution of the orbit. Orbital data must be accurate to at least the centimeter level in order to make accurate predictions of these forces.

Shown below are the relative magnitudes of three perturbing forces acting on ERS-1, the drag force (D), the lift force (L), and the radiation pressure force (R).

$$D = \frac{1}{2}\rho v^2 A C_D \tag{B.1}$$

$$D = \frac{1}{2}\left(7.628E - 15\frac{kg}{m^3}\right)\left(7500\frac{m}{s}\right)^2\left(36m^2\right)(4.5) = 3.476E - 5N \tag{B.2}$$

$$L = \frac{1}{2}\rho v^2 A C_L \tag{B.3}$$

$$L = \frac{1}{2}\left(7.628E - 15\frac{kg}{m^3}\right)\left(7500\frac{m}{s}\right)^2\left(36m^2\right)(1.0) = 7.772E - 6N \tag{B.4}$$

$$R = \nu C_R A P_s \tag{B.5}$$

$$R = (1)(0.083)\left(36.0m^2\right)\left(4.7E - 6\frac{N}{m^2}\right) = 1.40E - 5N \tag{B.6}$$

It is easily seen that the lift force is much smaller than the drag and radiation forces. This force is often neglected but as more accurate orbit predictions are required it is a force that should be considered.

Vita

Peter Demarest was born in Warrensburg, New York on December 29, 1971. He attended schools in Lake George and Bolton Landing, graduating in June 1990 from Bolton Central School. He received a Bachelor of Science Degree in Mechanical Engineering from Worcester Polytechnic Institute, Worcester Massachusetts in May 1994. In August of 1994 he began classes at the University of Tennessee Space Institute, Tullahoma Tennessee. He was awarded a Master of Science Degree in Aerospace Engineering from the University of Tennessee, Knoxville in August 1994.